

# QCD analysis of near-to-planar 3-jet events

---

**A. Banfi, G. Marchesini,**

*Dipartimento di Fisica, Università di Milano-Bicocca and INFN, Sezione di Milano, Italy*

**Yu.L. Dokshitzer,**

*LPT, Université de Paris XI, Centre d'Orsay, France* \*

**G. Zanderighi.**

*Dipartimento di Fisica, Università di Pavia and INFN, Sezione di Pavia, Italy*

**ABSTRACT:** Perturbative QCD analysis is presented of the cumulative out-of-plane momentum distribution in the near-to-planar  $e^+e^-$  annihilation events,  $K_{\text{out}} \ll Q$ . In this kinematical region multiple gluon radiation effects become essential. They are resummed with the single-logarithmic accuracy, which programme includes the 2-loop treatment of the basic radiation and matching with the exact  $\mathcal{O}(\alpha_s^2)$  result. Dedicated experimental analyses of 3-jet event characteristics are of special interest for the study of the non-perturbative confinement effects.

**KEYWORDS:** QCD, NLO Computations, Jets, LEP and SLC Physics.

---

\*on leave from PNPI, Gatchina, St. Petersburg, Russia

---

## Contents

<b>1. Introduction</b>	<b>2</b>
<b>2. Aplanarity and soft parton resummation</b>	<b>5</b>
2.1 Jet momenta and hard parton recoil	7
2.2 Kinematics of soft or collinear emission	9
2.3 Matrix element factorization	9
2.4 Phase space factorisation	11
<b>3. Right <math>K_{\text{out}}</math>-distribution</b>	<b>13</b>
<b>4. Total <math>K_{\text{out}}</math>-distribution</b>	<b>17</b>
4.1 Radiators in the quasi-2-jet limit	21
<b>5. Discussion and conclusions</b>	<b>23</b>
<b>A. Kinematics</b>	<b>24</b>
A.1 Kinematics of $q\bar{q}g$ jets	24
A.2 Born cross sections	26
A.3 Soft partons	27
<b>B. Radiators</b>	<b>27</b>
B.1 Integrating over $\alpha$	28
B.2 Integrating over $k_y$	29
B.2.1 Dipole 23	30
B.2.2 Dipoles 12 and 13	31
B.3 Radiator by assembling bits and pieces	32
B.4 Radiator for the right distribution	33
B.5 Running coupling	34
B.6 The sources and the $k_x$ integrals	34
<b>C. Evaluation of <math>\mathcal{F}</math></b>	<b>35</b>
C.1 $\mathcal{F}$ in the first order	36

---

## 1. Introduction

In recent years the standards were established for the perturbative QCD description of various characteristics of hadron jets produced in  $e^+e^-$  annihilation. These standards include:

- all-order resummation of double- (DL) and single-logarithmic (SL) contributions due to soft and collinear gluon radiation effects,
- two-loop analysis of the basic gluon radiation probability and
- matching the resummed logarithmic expressions with the exact  $\mathcal{O}(\alpha_s^2)$  results.

Such programmes were carried out for a number of jet shape observables such as Thrust ( $T$ ) and heavy jet mass ( $M_H$ ) [1],  $C$ -parameter [2] and jet Broadenings (total  $B_T$  and wide-jet broadening  $B_W$ ) [3].

Perturbative description of jets produced in processes other than  $e^+e^-$  annihilation poses more difficulties, as the structure of jets (both average jet characteristics and distributions) becomes sensitive to details of the underlying hard interaction. For example, characteristics of quark jets produced in the current fragmentation region in Deep Inelastic Scattering (DIS) depend on the Bjorken  $x$ . In spite of these complications a steady progress is being made in this domain as well [4].

Given a (relative) perfection of perturbative QCD technologies, it became possible to aim at *deviations* of the measured hadronic characteristics from the corresponding perturbative predictions, in a search for genuine non-perturbative confinement effects. As is well known, these deviations, for a broad variety of jet observables, amount to sizable  $1/Q$  corrections, with  $Q$  the hardness scale (the total  $e^+e^-$  annihilation energy), for reviews see [5, 6].

As far as physics of  $e^+e^-$  annihilation is concerned, till now these developments, both in the perturbative and non-perturbative sectors, were confined to two-jet ensembles which constitute the bulk of events. Little (if any) attention has been paid to multi-jet ensembles, in particular to three-jet events. In spite of being obviously more rare ( $\sigma_N/\sigma_{tot} \propto \alpha_s^{N-2}$ , with  $N$  the number of jets), selected multi-jet configurations are of special interest as they, so to speak, are subject to *more* quantum mechanics than unrestricted (mainly two-jet) hadron production events.

Indeed, in the latter case it is known that the gross inclusive features of particle production can be described in *probabilistic terms* by imposing *angular ordering* [7] on successive  $1 \rightarrow 2$  intra-jet parton decays. It suffices to implement *strict* angular ordering,  $\theta_{i+1} \leq \theta_i$ , the proper running coupling,  $\alpha_s(k_\perp)$ , and the standard parton splitting probabilities to ensure the *next-to-leading* accuracy of the perturbative description of inclusive energy spectra, mean multiplicities and the multiplicity distribution [8].

Thus, a transparent and powerful probabilistic technology exists for predicting (with next-to-leading accuracy) *inclusive* observables. At the same time, the very selection of events (say, three-jet events) necessarily makes a measurement “less inclusive” and destroys, generally speaking, the probabilistic picture, and one’s hold on the SL accuracy with it.

Of special interest for two-jet configurations is the kinematical region of two *narrow* jets ( $1 - T, M_H^2/Q^2, C, B_{T,W} \ll 1$ ) where multiple radiation (Sudakov suppression) effects are essential. An analogue of this region for three-jet events is near-to-planar kinematics. Three hard partons —  $q\bar{q}$  and a gluon  $g$  — form a plane. Secondary gluon radiation off the three-prong QCD antenna brings in aplanarity. In what follows we choose the out-of-plane transverse momentum  $K_{\text{out}}$  as an aplanarity measure. The distribution of events in  $K_{\text{out}}$  is subject to DL suppression in the region of small aplanarity,  $K_{\text{out}}/Q \ll 1$ , where normal accompanying radiation is vetoed.

The corresponding suppression factor, and thus the resulting  $K_{\text{out}}$ -distribution is easy to predict in a DL approximation which takes care of the leading contributions  $\mathcal{O}([\alpha_s \ln^2(Q/K_{\text{out}})]^n)$  in all orders while disregarding subleading SL corrections of the order of  $[\alpha_s \ln(Q/K_{\text{out}})]^m$ . The answer is given simply by the product of three proper QCD Sudakov factors,  $F_q^2 \cdot F_g$ , which veto radiation of gluons with out-of-plane momentum components exceeding  $K_{\text{out}}$ , off the three hard partons treated as independent emitters.

The DL approximation is known to be too rough to be practically reliable. Improving it proves to be nontrivial a quest: at the level of SL terms the *geometry* of the underlying three-jet configuration enters the game: in addition to *intra-jet* parton multiplication one has to take into consideration *inter-jet* particle production. The latter, however, does not admit “classical” probabilistic interpretation: gluon radiation in-between jets results from the coherent action of all three elements of the antenna.

This is a general feature which complicates the analyses of other, more simple, characteristics of three-jet ensembles as well. For example, contribution of coherent inter-jet particle flows enters, at the level of the next-to-leading  $\mathcal{O}(\sqrt{\alpha_s})$  correction, into perturbative prediction of the mean particle multiplicity in three-jet events, making it event-geometry-dependent [9].

In this paper we attempt, for the first time, the all-order perturbative analysis of the  $K_{\text{out}}$ -distribution in three-jet  $e^+e^-$  annihilation events, aiming at SL accuracy. In what follows we will single out and resum logarithmically-enhanced DL and SL contributions and systematically neglect relative corrections of the order  $\mathcal{O}(\alpha_s)$ . The latter belong to the non-logarithmic normalization factor (“coefficient function”)  $1 + c\alpha_s + \dots$ , whose first coefficient,  $c$ , can be found by comparing the approximate resummed result with numerical calculation based on the exact  $\alpha_s^2$  matrix element [10].

To accommodate all essential SL contributions one has

1. to take into account soft inter-jet gluon radiation,
2. to analyse corrections due to hard intra-jet parton decays,
3. to define an event plane for a multi-parton system and properly treat kinematical effects due to parton recoil,
4. to prove, for three-jet environment, soft gluon exponentiation (at the two-loop level) and the prescription for the argument of the running coupling that enters the basic gluon emission probability.

In the present paper we address these issues.

The answer we derive has the following key features:

- Kinematical constraints which determine an event plane are rather complicated but can be resolved with a help of multiple Fourier–Mellin representation which allows for exponentiation of multiple radiation in the parameter space.
- Multiple soft radiation off the three-parton system can be resummed and exponentiated in terms of three colour dipoles that together determine the colour structure of (and accompanying particle flows in) the event.
- For the cumulative  $K_{\text{out}}$ -distribution (as well as for other sufficiently inclusive observables) inclusive treatment of the two-parton decay of a gluon emitted by the  $q\bar{q}g$  system results in the running of the coupling constant.
- The running  $\alpha_s$  which describes the intensity of gluon emission off each dipole ( $qg$ ,  $\bar{q}g$ ,  $q\bar{q}$ ) depends on the invariant transverse momentum of the gluon with respect to two partons that form the corresponding dipole.
- The exponent can be represented as a sum of three basic parton “radiators” each of which describes one-gluon emission off a single hard parton, weighted by the colour factor of this parton. This radiation can be treated as independent provided a proper hardness scale is ascribed to the parton radiator.
- Essential SL contribution (“hard” intra-jet and coherent inter-jet corrections) can be conveniently embodied into the scales. Effects of the large-angle soft (inter-jet) radiation make these scales event-geometry-dependent and different for each of the three primary partons.
- The structure of the hardness scales of the parton radiators entering in the total  $K_{\text{out}}$ -distribution has a clear geometrical interpretation: the scale  $Q_a$  for the parton  $a$  is proportional to the invariant transverse momentum of this parton,  $p_{ta}$ , with respect to the hyper-plane formed by the other two hard partons.

- Equivalent expressions for the radiators of the total  $K_{\text{out}}$ -distributions can be constructed which smoothly interpolate between 3- and 2-jet configurations.

As has been already said, kinematics of three-jet observables complicates the analysis. As a result, the final expressions are rather cumbersome as they involve 4- and 5-dimensional integrals.

The kinematical constraints, and thus the final formulae, are somewhat simpler for the distribution of  $K_{\text{out}}$  accumulated in the *right* hemisphere, i.e. the one that has the smallest transverse momentum with respect to the thrust axis (for a review see [11]).

Quantitative analysis of the predictions and numerical results are discussed in a separate publication [10].

The paper is organised as follows.

In Section 2 we define the aplanarity measure  $K_{\text{out}}$ , derive kinematical relations defining the event plane and discuss resummation of soft gluon radiation for near-to-planar 3-jet events.

Section 3 is devoted to perturbative analysis of the  $K_{\text{out}}$ -distribution in the right hemisphere. Here we develop technique for analysing and embodying all necessary SL corrections into the all-order perturbative result.

In Section 4 we apply this technique to derive, with SL accuracy, the perturbative prediction for the total  $K_{\text{out}}$ -distribution in 3-jet events with given kinematics (thrust  $T$  and thrust-major  $T_M$ ).

Technical details are confined to Appendices.

## 2. Aplanarity and soft parton resummation

We consider  $e^+e^-$  annihilation events with almost planar configuration of final state particles. Such event are characterised by the inequality

$$T \sim T_M \gg T_m , \quad (2.1)$$

with  $T$  the thrust,  $T_M$  and  $T_m$  the so-called thrust-major and thrust-minor. We study the distribution of  $T_m$ . We shall refer to  $e^+e^-$  events in this phase space region as 3-jet events.

Thrust is defined as

$$T Q = \max_{\vec{n}} \left\{ \sum_h |\vec{n} \vec{p}_h| \right\} = \sum_h |\vec{n}_T \vec{p}_h| = \sum_h |p_{hz}| , \quad (2.2)$$

where the sum runs over all particles  $h$  produced in a given event with the total center of mass energy  $Q$ . Hereafter we choose the  $z$ -axis to lie along the thrust axis,

$\vec{n}_T$ . The thrust-major is defined analogously; it maximises the sum of the particle momenta projections in the two-dimensional plane orthogonal to the thrust axis:

$$T_M Q = \max_{\vec{n}\vec{n}_T=0} \left\{ \sum_h |\vec{n}\vec{p}_h| \right\} = \sum_h |\vec{n}_M \vec{p}_h| = \sum_h |p_{hy}| . \quad (2.3)$$

The direction  $\vec{n}_M$  we shall identify with the  $y$ -axis. Finally, for the thrust-minor we have

$$T_m Q = \sum_h |p_{hx}| \equiv K_{\text{out}} . \quad (2.4)$$

We choose  $\vec{n}_T$  in such a way that the most energetic particle in the event has a positive  $z$ -component and  $\vec{n}_M$  in such a way that the second most energetic particle has a positive  $y$ -component. Hereafter we attribute  $p_h$  to the **right** hemisphere  $C_R$  (**left** hemisphere  $C_L$ ) if  $p_{hz} > 0$  ( $p_{hz} < 0$ ). Similarly  $p_h$  is in the **up** hemisphere  $C_U$  (**down** hemisphere  $C_D$ ) if  $p_{hy} > 0$  ( $p_{hy} < 0$ ). We shall also consider separately the right-hemisphere cumulative out-of-plane transverse momentum:

$$K_{\text{out}}^R \equiv \sum_{h \in R} |p_{hx}| . \quad (2.5)$$

It can be easily shown that from the definition (2.2–2.3) the kinematical constraints follow:

$$\sum_{h \in R} \vec{p}_{ht} = \sum_{h \in L} \vec{p}_{ht} = 0 , \quad \sum_{h \in U} p_{hx} = \sum_{h \in D} p_{hx} = 0 , \quad (2.6)$$

where  $\vec{p}_t$  is the two-dimensional vector transversal to the  $z$ -axis. We introduce the three-dimensional vector  $\vec{P}_1$  and the two-dimensional vector  $\vec{P}_{2t}$  that define the “event plane”  $\{z, y\}$ :

$$\vec{P}_1 = (P_{1x}, P_{1y}, P_{1z}) = (0, 0, TE) , \quad \vec{P}_{2t} = (P_{2x}, P_{2y}) = (0, T_M E) , \quad Q = 2E . \quad (2.7)$$

From the definition of  $T$  and  $T_M$  we have

$$\vec{P}_1 = \sum_{h \in R} \vec{p}_h , \quad \vec{P}_{2t} = \sum_{h \in U} \vec{p}_{ht} . \quad (2.8)$$

In what follows we study the distribution of events in the cumulative out-of-plane transverse momentum  $K_{\text{out}}$  defined in (2.4). The integrated  $K_{\text{out}}$ -distribution is defined as

$$\frac{d\sigma(K_{\text{out}})}{dT dT_M} = Q^5 \sum_m \int d\sigma_m \Theta \left( K_{\text{out}} - \sum_{h=1}^m |p_{hx}| \right) \delta^3 \left( \sum_{h \in R} \vec{p}_h - \vec{P}_1 \right) \delta^2 \left( \sum_{h \in U} \vec{p}_{ht} - \vec{P}_{2t} \right) , \quad (2.9)$$

where  $m$  denotes the number of final particles in an event. The last two delta-functions fix the event plane and the theta-function defines the observable. Analogously we define the *right* distribution by restricting the sum over particles in the theta-function of (2.9) to those belonging to the right hemisphere (see (2.5)).

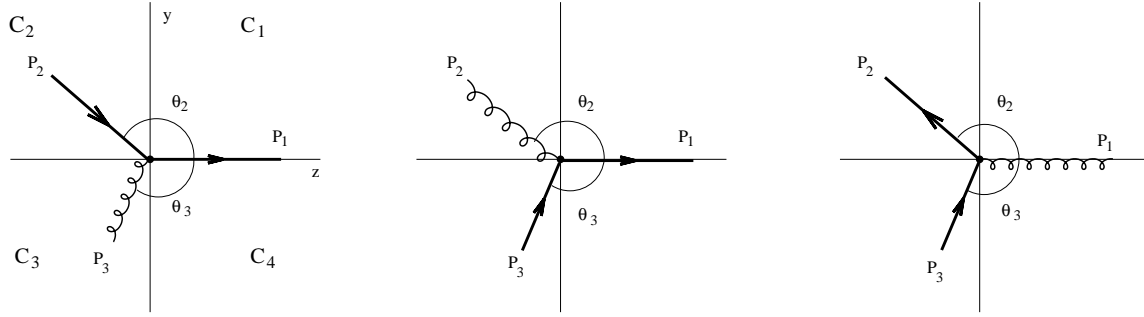


**Figure 1:** The three Born configurations  $\mathcal{C}_3, \mathcal{C}_2$  and  $\mathcal{C}_1$  for  $T = 0.75$  and  $T_M = 0.48$  ordered according to decreasing probability. The thrust  $T$  and thrust major  $T_M$  are along the  $z$ - and  $y$ -axis respectively. The four regions  $\mathcal{C}_\ell$  in the phase space are indicated.

## 2.1 Jet momenta and hard parton recoil

At the parton level the events in the region (2.1) can be treated as three-jet events generated by a system of energetic quark, antiquark and a gluon accompanied by an ensemble of soft partons.

At the Born level,  $\mathcal{O}(\alpha_s)$ , in the absence of accompanying radiation the 3-parton system is truly planar,  $T_m \equiv 0$ . The kinematical configuration of  $q, \bar{q}$  and  $g$  treated as massless partons is then uniquely fixed by the values of  $T$  and  $T_M$ . Denoting by  $P_1, P_2$  and  $P_3$  the energy ordered parton momenta,  $P_{10} > P_{20} > P_{30}$ , we have  $\vec{P}_1$  lying along the thrust axis. The vectors  $\vec{P}_1$  and  $\vec{P}_{2t} = -\vec{P}_{3t}$  are given by the event plane momenta defined in (2.7).

There are various kinematical configurations of the Born system. The three parton momenta  $P_q, P_{\bar{q}}, P_g$  can belong to three configurations  $\mathcal{C}_\delta$ , namely (see Figure 1)

$$\begin{aligned} (P_1, P_2, P_3) &= (P_g, P_q, P_{\bar{q}}) \Rightarrow \mathcal{C}_1 \\ &= (P_q, P_g, P_{\bar{q}}) \Rightarrow \mathcal{C}_2 \\ &= (P_q, P_{\bar{q}}, P_g) \Rightarrow \mathcal{C}_3. \end{aligned} \quad (2.10)$$

Notice that the index  $\delta$  labelling the configuration  $\mathcal{C}_\delta$  coincides with the index of the gluon momentum. (Interchanging the quark and the antiquark does not affect the accompanying radiation and the distributions under study.) For three massless partons the values of  $T$  and  $T_M$  are restricted to the region

$$\frac{2(1-T)}{T} \sqrt{2T-1} < T_M < \sqrt{1-T}. \quad (2.11)$$

(For the kinematics of the Born system momenta see Appendix A.) In the following we will analyse the distribution inside this region — the 3-jet region — in which three skeleton parton momenta  $P_a$  can be reconstructed from the  $T$  and  $T_M$  values.

Beyond the Born approximation, in the presence of secondary gluon radiation,  $T_m$  is no longer vanishing. The  $x$ -components of bremsstrahlung gluon momenta are logarithmically distributed over a broad range, so that  $\langle T_m \rangle \sim \alpha_s T_M \sim \alpha_s T$ .

In the region (2.1) the PT expansion develops logarithmically enhanced contributions which need to be resummed in all orders. Our aim is to perform this resummation with SL accuracy. This means that we shall keep both DL,  $\alpha_s \log^2 T_m$ , and SL,  $\alpha_s \log T_m$ , contributions to the exponent (“radiator”, see below) while neglecting non-logarithmic corrections  $\mathcal{O}(\alpha_s)$ . With account of the running coupling effect, the DL and SL contributions formally expand into series of terms  $\alpha_s^n \log^{n+1} T_m$  and  $\alpha_s^n \log^n T_m$ , respectively.

It is important to stress that exponentiation of the SL correction  $\alpha_s \log T_m$  makes sense only if it is supported by the calculation of the non-logarithmic “coefficient function”. Indeed, a “cross-talk” between an  $\mathcal{O}(\alpha_s)$  correction to the overall normalization of the resummed distribution and the leading DL term, symbolically,

$$(1 + c \cdot \alpha_s) \times \exp \{ \alpha_s \log^2 + s \cdot \alpha_s \log \} = 1 + \dots + c \cdot \alpha_s \times \alpha_s \log^2 + \frac{s^2}{2!} (\alpha_s \log)^2 + \dots , \quad (2.12)$$

gives rise to the correction of the same order as the SL term squared. The coefficient  $c$  is not known analytically. It can be determined by comparing the  $\mathcal{O}(\alpha_s^2)$  term of the log-resummed expression with the result of a numerical calculation based on the exact  $\alpha_s^2$  matrix element [10].

We denote by  $p_a$  the momenta of the three hard partons,  $q, \bar{q}, g$ , that in general no longer lie in the event plane defined by the vectors (2.7). In the region (2.1) they differ from  $P_a$  by “soft recoil parts”  $q_a$ ,

$$p_a = P_a + q_a , \quad (2.13)$$

whose  $x$ -components contribute to  $K_{\text{out}}$  together with the soft parton momenta  $k_i$ :

$$K_{\text{out}} = |q_{1x}| + |q_{2x}| + |q_{3x}| + \sum |k_{ix}| . \quad (2.14)$$

To SL accuracy, as in the case of the broadening distribution [3], it suffices to keep the recoil momenta  $q_a$  only in the phase space, in particular their contribution to  $K_{\text{out}}$  and to the constraints defining the event plane (see (2.9)). At the same time,  $q_a$  can be neglected in the radiation matrix element, that is, in the emission distributions we can substitute the skeleton momenta  $P_a$  for actual parton momenta  $p_a$ . We remark that, as in the case of jet broadening [12], for the study of *non-perturbative* power-suppressed corrections the approximation  $p_a \rightarrow P_a$  in the radiation matrix element is not valid [13].

In order to resum the PT series for (2.9) in the region (2.1) we need to use the factorization property of the soft radiation matrix element and to factorize the multi-parton phase space. We discuss these points in succession after giving a brief description of the kinematics. For more details see Appendix A.

## 2.2 Kinematics of soft or collinear emission

Introducing the recoil momenta  $q_a$  defined in (2.13), the right, left and total  $K_{\text{out}}$  are given by

$$K_{\text{out}}^R = |q_{1x}| + \sum_R |k_{ix}|, \quad K_{\text{out}}^L = |q_{2x}| + |q_{3x}| + \sum_L |k_{ix}|, \quad K_{\text{out}} = K_{\text{out}}^R + K_{\text{out}}^L. \quad (2.15)$$

The event plane momenta (2.7) are given by

$$\vec{P}_1 = \vec{p}_1 + \sum_R \vec{k}_i, \quad \vec{P}_{2t} = \vec{p}_{2t} + \vec{p}_{1t} \vartheta(p_{1y}) + \sum_U \vec{k}_{it}. \quad (2.16)$$

In the region in which the emitted partons are soft or collinear the components of  $q_a$  that accompany *non-vanishing* components of  $P_a$  can be neglected in the calculation. Therefore we consider only those four components that vanish in the Born approximation namely, the  $y$ -component of the leading parton momentum,  $q_{1y} = p_{1y}$ , and the  $x$ -components  $q_{ax} = p_{ax}$ ,  $a = 1, 2, 3$ . Then, from the kinematical relations (2.16) and (2.5) we have

$$\begin{aligned} q_{1y} + \sum_R k_{iy} &= q_{1x} + \sum_R k_{1x} = 0, \\ q_{2x} + q_{1x}^+ + \sum_U k_{1x} &= q_{3x} + q_{1x}^- + \sum_D k_{1x} = 0, \quad q_{1x}^\pm = q_{1x} \vartheta(\pm q_{1y}). \end{aligned} \quad (2.17)$$

Notice that this implies the following kinematical relations

$$\{q_{1x}^+ + \sum_{i \in C_1} k_{ix}\} = -\{q_{1x}^- + \sum_{i \in C_4} k_{ix}\} = -\{q_{2x} + \sum_{i \in C_2} k_{ix}\} = \{q_{3x} + \sum_{i \in C_3} k_{ix}\}. \quad (2.18)$$

## 2.3 Matrix element factorization

At the parton level the distribution is given by the sum of the partial cross sections

$$d\sigma_n = \frac{1}{n!} M_n^2 \cdot d\Phi_n, \quad (2.19)$$

where  $M_n$  is the matrix element for the emission of  $n$  secondary partons off the  $q\bar{q}$ ,  $g$  system, and  $d\Phi_n$  the corresponding phase-space factor,

$$d\Phi_n = (2\pi)^4 \delta^4 \left( \sum_a p_a + \sum_i k_i - Q \right) \prod_{i=1}^n [dk_i] \cdot \prod_{a=1}^3 \frac{d^3 p_a}{(2\pi)^3 2E_a}, \quad [dk] = \frac{d^3 k}{\pi \omega}. \quad (2.20)$$

As it is explained in detail in Appendix B.2.2 the contribution of collinear non soft emission is process independent and can be taken into account *a posteriori* introducing in the computed distribution the hard part of the splitting functions.

Therefore the accompanying partons  $k_i$  are assumed to be soft and their distribution can be treated as independent. Assembling together the contributions from the three configurations  $\mathcal{C}_\delta$  defined in (2.10), the distribution can be presented as

$$M_n^2 = \sum_{\delta=1}^3 M_0^2(\mathcal{C}_\delta) \cdot \prod_i^n W_\delta(k_i), \quad (2.21)$$

where  $M_0(\mathcal{C}_\delta)$  is the Born  $q\bar{q}g$  matrix element and  $W_\delta$  is the distribution of the soft gluon radiation off the hard three-parton antenna in the momentum configuration  $\mathcal{C}_\delta$ . Here we discuss the real emission contribution to  $M_n$ ; the virtual corrections will be accommodated later.

For the configuration  $\delta = 3$ , for example, the squared Born matrix element reads

$$M_0^2(\mathcal{C}_3) = \frac{C_F \alpha_s}{2\pi} \frac{x_1^2 + x_2^2}{(1-x_1)(1-x_2)}, \quad x_a \equiv \frac{2P_a Q}{Q^2}, \quad (2.22)$$

where  $P_3$  is the gluon momentum and  $P_1, P_2$  the quark-antiquark momenta (see (2.10)). For this configuration the single soft gluon radiation pattern is given, at the one-loop level, by

$$W_3(k) = C_F w_{12} + \frac{N_c}{2} (w_{13} + w_{23} - w_{12}) = \frac{N_c}{2} \left( w_{13} + w_{23} - \frac{1}{N_c^2} w_{12} \right). \quad (2.23)$$

Here  $w_{ab}$  is the standard two-parton antenna of the  $ab$ -dipole, which, within the normalization convention prescribed by (2.20), is given by

$$w_{ab}(k) = \frac{\alpha_s}{\pi} \frac{(P_a P_b)}{2(P_a k)(k P_b)} = \frac{\alpha_s}{\pi k_{t,ab}^2}. \quad (2.24)$$

Here  $k_{t,ab}$  is the invariant gluon transverse momentum with respect to the hyper-plane defined by the  $P_a, P_b$  momenta.

The first term  $C_F w_{12}$  in (2.23) is the “Abelian” contribution describing soft gluon emission off the  $q\bar{q}$  pair. The second term proportional to  $N_c$  is its “non-Abelian” counterpart that describes radiation off the hard gluon  $P_3$ . Similar expressions for two other kinematical configurations ( $\delta = 1, 2$ ) is straightforward to write down by properly adjusting the parton indices,

$$\begin{aligned} W_1(k) &= \frac{N_c}{2} \left( w_{13} + w_{12} - \frac{1}{N_c^2} w_{23} \right), \\ W_2(k) &= \frac{N_c}{2} \left( w_{23} + w_{12} - \frac{1}{N_c^2} w_{13} \right). \end{aligned} \quad (2.25)$$

To reach SL accuracy it is necessary to treat multi-parton emission at the two-loop level. This involves allowing secondary gluon to split into two gluons or into a  $q\bar{q}$  pair. In principle, perturbative analysis of a system consisting of three hard partons

and two softer partons (with comparable energies) can be found in the literature (see, e.g., [14]). However, to the best of our knowledge, the most important feature of the result has never been explicitly stressed, namely, that the colour structure and geometrical properties of emission of a soft two-parton system off a 3-jet ensemble is *identical* to those for single gluon radiation.

It can be shown [15] that after subtracting the uncorrelated radiation of two soft gluons,  $W_3(k_1)W_3(k_2)$ , the correlated two-parton production is given by the expression

$$W_3^{(2)}(k_1, k_2) = C_F w_{12}^{(2)}(k_1, k_2) + \frac{N_c}{2} \left( w_{13}^{(2)}(k_1, k_2) + w_{23}^{(2)}(k_1, k_2) - w_{12}^{(2)}(k_1, k_2) \right), \quad (2.26)$$

where  $w_{ab}^{(2)}$  is the standard distribution known from the two-loop analysis of 2-jet event shapes (the first term on the right-hand side of (2.26), see [16]). It describes decay into  $q\bar{q}$ - or  $gg$ -pair of a virtual parent gluon radiated, in our case, by one of the three two-parton dipoles  $ab$ . Given this remarkably simple dipole structure, the analysis of the two-loop effects in 3-jet events reduces to the known 2-jet case.

As shown in Ref. [16], for a sufficiently inclusive observable (and the  $K_{\text{out}}$ -distribution under interest in particular) the two-loop refinement results in (and reduces to) substituting the proper argument for the running coupling describing the intensity of the parent gluon emission,

$$w_{ab}(k) = \frac{\alpha_s}{\pi k_{t,ab}^2} \implies w_{ab}(k) + \int dk_1 dk_2 \delta(k - k_1 - k_2) w_{ab}^{(2)}(k_1, k_2) \simeq \frac{\alpha_s(k_{t,ab})}{\pi k_{t,ab}^2}. \quad (2.27)$$

Here  $k_{t,ab}$  is the invariant transverse momentum defined in (2.24) and  $\alpha_s$  is taken in the physical scheme [17]. It is worthwhile to notice that the arguments of the coupling are different for the three dipoles that participate in gluon radiation according to (2.23).

We remark that at the level of the leading power-suppressed *non-perturbative* correction the rôle of two-loop effects is more involved as they give rise to the Milan factor [6, 16, 18].

## 2.4 Phase space factorisation

We discuss here factorization of the phase space in the soft region, which is needed for resummation. The phase space factor reads

$$\begin{aligned} d\Gamma_n &= d\Phi_n \cdot \delta^3\left(\vec{p}_1 + \sum_R \vec{k}_i - \vec{P}_1\right) \delta^2\left(\vec{p}_{2t} + \vec{p}_{1t} \vartheta(p_{1y}) + \sum_U \vec{k}_{it} - \vec{P}_{2t}\right) \\ &= \prod_{i=1}^n [dk_i] \cdot \prod_{a=1}^3 \frac{d^3 p_a}{(2\pi)^3 2E_a} \cdot D_n, \quad [dk] = \frac{d^3 k}{\pi \omega}, \end{aligned} \quad (2.28)$$

where the factor  $D_n$  takes care of the kinematical relations,

$$D_n = (2\pi)^4 \delta^4 \left( \sum_a p_a + \sum_i k_i - Q \right) \delta^3 \left( \vec{p}_1 + \sum_R \vec{k}_i - \vec{P}_1 \right) \delta^2 \left( \vec{p}_{2t} + \vec{p}_{1t} \vartheta(p_{1y}) + \sum_U \vec{k}_{it} - \vec{P}_{2t} \right). \quad (2.29)$$

The first delta-function stands for the energy–momentum conservation, while the last two (three- and two-dimensional) delta-functions set the event plane.

Now we single out from  $d\Gamma_n$  small recoil components of hard partons momenta,  $q_{1y} = p_{1y}$  and the three  $q_{ax} = p_{ax}$ , which have to satisfy four event-plane constraints given in (2.17). Then, introducing the unity,

$$1 = \int dq_{1y} \prod_a dq_{ax} \cdot S_n,$$

where

$$S_n \equiv \delta \left( q_{1y} + \sum_R k_{iy} \right) \delta \left( q_{1x} + \sum_R k_{ix} \right) \delta \left( q_{2x} + q_{1x}^+ + \sum_U k_{ix} \right) \delta \left( q_{3x} + q_{1x}^- + \sum_D k_{ix} \right), \quad (2.30)$$

we neglect hard parton recoils  $q_{ai}$  in all but these four components and approximate the kinematical factor  $D_n$  as follows

$$D_n = \int dq_{1y} \prod_a dq_{ax} S_n \cdot D_n \simeq D_0 \cdot \int dq_{1y} \prod_a dq_{ax} \cdot S_n. \quad (2.31)$$

Here  $D_0$  is a trivial phase space factor which corresponds to the Born three-parton kinematics,

$$D_0 = (2\pi)^4 \delta^4 \left( \sum_a p_a - Q \right) \delta^3 \left( \vec{p}_1 - \vec{P}_1 \right) \delta^2 \left( \vec{p}_{2t} - \vec{P}_{2t} \right).$$

We then have

$$d\Gamma_n \simeq \Gamma_0 \prod_{i=1}^n [dk_i] dh_n, \quad dh_n = dq_{1y} \prod_{a=1}^3 dq_{ax} \cdot S_n, \quad \Gamma_0 = \prod_{a=1}^3 \frac{d^3 p_a}{(2\pi)^3 2E_a} \cdot D_0, \quad (2.32)$$

where  $\Gamma_0$  is the Born phase space given in Appendix A.

Neglecting bremsstrahlung in the  $D_0$ -factor proves to be legitimate: it can be shown that to achieve SL accuracy it suffices to take care of accompanying parton momenta in the  $S$ -factor (2.30) and in the observable itself.

Finally, in order to “exponentiate” the multiple radiation we need to factorize dependence on individual secondary parton momenta contained in the delta-functions

in  $S_n$  and in the  $K_{\text{out}}$ -observable. This is achieved in a standard way by means of Mellin and Fourier representations. In the following we apply this procedure to the integrated  $K_{\text{out}}$ -distribution defined in (2.9).

In what follows we shall separately consider  $K_{\text{out}}$  accumulated in the right hemisphere and the total  $K_{\text{out}}$  of the event. We start from a simpler case of the  $K_{\text{out}}$ -distribution in the *right* (one-jet) hemisphere. The total  $K_{\text{out}}$ -distributions will be considered in Sec. 4.

### 3. Right $K_{\text{out}}$ -distribution

Consider the differential three-jet cross section with given  $T$  and  $T_M$  and with accumulated out-of-event-plane momentum in the right hemisphere smaller than a given  $K_{\text{out}}$ . Using the soft-factorization formula (2.21) we can write the cross section (2.9) for small  $K_{\text{out}}$  in the form

$$\begin{aligned} \frac{d\sigma^R(K_{\text{out}})}{dTdT_M} &= \sum_n \frac{1}{n!} \int M_n^2 d\Gamma_n \vartheta \left( K_{\text{out}} - |q_{1x}| - \sum_R |k_{ix}| \right) \\ &= \sum_{\delta=1}^3 \frac{d\sigma_{\delta}^{(0)}}{dTdT_M} \cdot \Sigma_{\delta}^R(K_{\text{out}}), \end{aligned} \quad (3.1)$$

where  $\sigma_{\delta}^{(0)}$  is the three-jet differential Born cross section for the parton configuration  $\mathcal{C}_{\delta}$  defined in (2.10),

$$\frac{d\sigma_{\delta}^{(0)}}{dTdT_M} \equiv \Gamma_0 M_0^2(\mathcal{C}_{\delta}),$$

calculated in Appendix A. The accompanying radiation factor  $\Sigma$ , a function of  $K_{\text{out}}$ ,  $T$  and  $T_M$ , reads

$$\begin{aligned} \Sigma_{\delta}^R(K_{\text{out}}) &= \int \sum_n \frac{1}{n!} \prod_i^n [dk_i] W_{\delta}(k_i) \cdot H^R(K_{\text{out}}), \\ H^R(K_{\text{out}}) &\equiv \int dh_n \vartheta \left( K_{\text{out}} - |q_{1x}| - \sum_R |k_{ix}| \right). \end{aligned} \quad (3.2)$$

We recall that within the adopted PT accuracy the hard parton momenta  $p_a$  entering into the soft gluon distribution factor  $W_{\delta}(k)$  can be approximated by the event plane vectors  $P_a$  so that integration over the recoil variables  $q_a = p_a - P_a$  can be easily performed. Since the observable involves only momenta in the right hemisphere, the recoil momentum components in the left hemisphere  $q_{2x}$  and  $q_{3x}$  can be freely integrated out with use of the last two delta-functions in (2.30) and leave no trace in the distribution under consideration. Then, a non-trivial dependence on  $q_{1y}$  (via

$q_{1x}^\pm)$  also disappears, and the  $q_{1y}$ -integration trivializes as well. We are left with a single delta-function in (2.30):

$$H^R(K_{\text{out}}) = \int dq_{1x} \vartheta \left( K_{\text{out}} - |q_{1x}| - \sum_R |k_{ix}| \right) \delta \left( q_{1x} + \sum_R k_{ix} \right).$$

To factorize the dependence on secondary parton momenta we use the Mellin representation for the theta-function in  $K_{\text{out}}$  and the Fourier representation for the delta-function in  $q_{1x}$ :

$$\vartheta \left( K_{\text{out}} - |q_{1x}| - \sum_R |k_{ix}| \right) = \int_{\mathcal{C}} \frac{d\nu}{2\pi i \nu} \exp \left\{ \nu \cdot \left( K_{\text{out}} - |q_{1x}| - \sum_R |k_{ix}| \right) \right\} \quad (3.3)$$

$$\delta \left( q_{1x} + \sum_R k_{ix} \right) = \nu \int_{-\infty}^{\infty} \frac{d\beta}{2\pi} \exp \left\{ -i\nu \beta \cdot \left( q_{1x} + \sum_R k_{ix} \right) \right\}, \quad (3.4)$$

where the contour  $\mathcal{C}$  in (3.3) runs parallel to the imaginary axis at  $\text{real} \nu > 0$ . Defining the Fourier integral (3.4) we have extracted, for the sake of convenience, the factor  $\nu$  as if it were a real parameter: for a complex value of  $\nu$  it implies rotating the  $\beta$ -contour by  $-\text{Arg} \nu$ ,  $|\text{Arg} \nu| < \pi/2$ . (Then, using the analytic continuation, the  $\beta$ -integral can be transformed to run along the real axis.)

Integrating over  $q_{1x}$  we obtain

$$H^R(K_{\text{out}}) = \int_{\mathcal{C}} \frac{d\nu}{2\pi i \nu} e^{\nu K_{\text{out}}} \int_{-\infty}^{\infty} \frac{d\beta}{\pi(1 + \beta^2)} \cdot \prod_R e^{-\nu(|k_{ix}| + i\beta k_{ix})}. \quad (3.5)$$

The limit of small  $K_{\text{out}}$  (and thus of small  $q_{1x}$ ) corresponds to the region of large values of the conjugate variables, i.e.  $\nu$  and  $\nu\beta$  respectively. Therefore in what follows we will concentrate on the limit of large  $\nu$  and neglect the contributions of the order of  $\nu^{-1}$  which correspond to  $\mathcal{O}(K_{\text{out}})$  corrections to the distribution. At the same time, by examining (3.5) it is easy to see that the characteristic values of the rescaled Fourier variable  $\beta$  are of the order of unity.

Substituting (3.5) into (3.2) we get

$$\Sigma_{\delta}^R(K_{\text{out}}) = \int_{\mathcal{C}} \frac{d\nu}{2\pi i \nu} e^{\nu K_{\text{out}}} \int_{-\infty}^{\infty} \frac{d\beta}{\pi(1 + \beta^2)} e^{-\mathcal{R}_{\delta}^R(\nu, \beta)}, \quad (3.6)$$

where we have introduced the ‘‘radiator’’

$$\mathcal{R}_{\delta}^R(\nu, \beta) = \int_R [dk] W_{\delta}(k) \left[ 1 - e^{-\nu(|k_x| + i\beta k_x)} \right]. \quad (3.7)$$

Here the unity in the square brackets has been included to account for the virtual corrections.

For example, for the most probable jet configuration  $\delta = 3$  (with gluon the least energetic parton), the soft distribution (2.23) gives

$$\mathcal{R}_3^R = \frac{N_c}{2} \left( r_{13}^R + r_{23}^R - \frac{1}{N_c^2} r_{12}^R \right), \quad r_{ab}^R = \int_R [dk] w_{ab}(k) \left[ 1 - e^{-\nu(|k_x| + i\beta k_x)} \right]. \quad (3.8)$$

With the DL accuracy only gluons collinear to  $P_1$  (the thrust axis direction) contribute to the right-hemisphere  $K_{\text{out}}$ . Therefore the (identical) DL contributions are contained in  $r_{12}^R$  and  $r_{13}^R$ . According to (3.8), they combine into the expression proportional to  $C_F$  — the colour charge of the quark  $P_1$ . Single logarithmic corrections to these two dipoles, as well as SL contribution of the third dipole,  $r_{23}^R$ , are calculated in Appendix B.4. Here we report the result:

$$r_{1a}^R = r(\bar{\mu}, Q^2) + F_{1a} \int_{1/\bar{\mu}}^Q \frac{dk_x}{k_x} \frac{\alpha_s(2k_x)}{\pi}, \quad r_{23}^R = F_{23} \int_{1/\bar{\mu}}^Q \frac{dk_x}{k_x} \frac{\alpha_s(2k_x)}{\pi}, \quad (3.9)$$

where the variable  $\bar{\mu}$  originates from an approximate evaluation of the characteristic momentum integral which is explained in Appendix B.6,

$$\left[ 1 - e^{\nu(|k_x| + i\beta k_x)} \right] \rightarrow \theta \left( |k_x| - \frac{1}{\bar{\mu}} \right), \quad \bar{\mu} = \bar{\nu} \mu, \quad \mu = \sqrt{1 + \beta^2}, \quad (3.10)$$

with

$$\bar{\nu} \equiv \nu e^{\gamma_E}. \quad (3.11)$$

In (3.9)  $r(\bar{\mu}, Q^2)$  is the DL function

$$r(\bar{\mu}, Q'^2) = \int_{1/\bar{\mu}}^{Q'} \frac{dk_x}{k_x} \frac{\alpha_s(2k_x)}{\pi} \ln \frac{Q'^2}{k_x^2}, \quad (3.12)$$

and the factors  $F_{ab} = F_{ab}(T, T_M)$  are independent of the integration variables  $\nu$  and  $\beta$ . The origin of an essential subleading correction embodied into the precise argument of the running coupling,  $\alpha_s(2k_x)$ , is explained in Appendix B.5.

Combining these results we obtain the radiators, evaluated with SL accuracy, for each of the three kinematical jet configurations,

$$\mathcal{R}_\delta^R(\bar{\mu}) = C_\delta r(\bar{\mu}, Q_\delta^2). \quad (3.13)$$

Here  $C_\delta$  is the colour charge of the hard parton along the thrust axis, that is  $C_\delta = C_F$  for  $\delta = 2, 3$  and  $C_1 = N_c$ . SL corrections in (3.13) were absorbed into the definition of the hard scale. The corresponding scale  $Q_\delta$  depends on the event configuration  $\delta$  and, though the functions  $F_{ab}(T, T_M)$ , on the event kinematics. These scales are

given by

$$\begin{aligned}
N_C \ln Q_1^2 &= N_C \ln(Q^2 e^{-\frac{\beta_0}{2N_c}}) + \frac{N_c}{2} (F_{12} + F_{13} - \frac{1}{N_c^2} F_{23}), \\
C_F \ln Q_2^2 &= C_F \ln(Q^2 e^{-\frac{3}{2}}) + \frac{N_c}{2} (F_{12} + F_{23} - \frac{1}{N_c^2} F_{13}), \\
C_F \ln Q_3^2 &= C_F \ln(Q^2 e^{-\frac{3}{2}}) + \frac{N_c}{2} (F_{13} + F_{23} - \frac{1}{N_c^2} F_{12}).
\end{aligned} \tag{3.14}$$

They also include the factors  $e^{-3/4}$  and  $e^{-\beta_0/4N_c}$  coming from SL corrections due to the “hard” parts of the quark and gluon splitting functions. As we shall see below in Sec. 4, for the case of the *total*  $K_{\text{out}}$ -distribution the corresponding scales are simply related with geometry of the 3-jet event. At the same time, the  $T$ - and  $T_M$ -dependence of the scales entering into one-hemisphere distribution does not have a simple geometrical interpretation. This is due to the fact that the kinematical constraint restricting the observable to a single hemisphere is foreign to the structure of the soft-gluon radiation pattern.

The radiator (3.13) depends on the Mellin-Fourier moments  $\nu$  and  $\beta$  only via the variable  $\bar{\nu}$ . The  $\beta$ -dependence can be further simplified at SL accuracy by expanding the radiator for large  $\nu$ ,

$$\mathcal{R}_\delta^R(\bar{\mu}) = \mathcal{R}_\delta^R(\bar{\nu}) + C_\delta r'(\bar{\nu}) \ln \sqrt{1 + \beta^2},$$

where

$$r'(\bar{\nu}) = \frac{\alpha_s(k_x)}{\pi} \ln \frac{Q^2}{k_x^2}, \quad k_x \equiv 1/\bar{\nu}. \tag{3.15}$$

Since  $r'$  constitutes a SL correction, we can use  $Q$  as a common scale (neglecting  $\mathcal{O}(\alpha_s)$  mismatch) and omit the factor 2 in the running coupling argument (as producing a negligible correction  $\mathcal{O}(\alpha_s^2 \log \bar{\nu})$ ) in such subleading terms.

Thus, the right-hemisphere  $K_{\text{out}}$ -distribution to SL accuracy takes the form

$$\begin{aligned}
\Sigma_\delta^R(K_{\text{out}}) &= \int \frac{d\nu}{2\pi i\nu} e^{\nu K_{\text{out}}} e^{-\mathcal{R}_\delta^R(\bar{\nu})} \mathcal{F}_\delta^R(\bar{\nu}), \\
\mathcal{F}_\delta^R(\bar{\nu}) &= \int_{-\infty}^{\infty} \frac{d\beta}{\pi(1 + \beta^2)^{1+\eta}} = \frac{\Gamma(\frac{1}{2} + \eta)}{\sqrt{\pi}\Gamma(1 + \eta)}, \quad \eta = \frac{1}{2}C_\delta r'(\bar{\nu}).
\end{aligned} \tag{3.16}$$

Integration over the Mellin variable  $\nu$  can be performed by steepest descent or by the operator method introduced in [12]. We follow the last method which exploits the following identities:

$$\begin{aligned}
f(\bar{\nu}) &= f(e^{-\partial_z}) \cdot (\bar{\nu})^{-z} \Big|_{z=0}; \\
\int \frac{d\nu}{2\pi i\nu} (\bar{\nu})^{-z} e^{\nu K_{\text{out}}} &= \frac{(\bar{K}_{\text{out}})^z}{\Gamma(1 + z)}, \quad \bar{K}_{\text{out}} \equiv e^{-\gamma_E} K_{\text{out}}.
\end{aligned}$$

The following approximation is valid:

$$e^{-R(e^{-\partial_z})} \mathcal{F}(e^{-\partial_z}) \frac{(\bar{K}_{\text{out}})^z}{\Gamma(1+z)} \Big|_{z=0} \simeq e^{-R(\bar{K}_{\text{out}}^{-1})} \mathcal{F}(\bar{K}_{\text{out}}^{-1}) \cdot \Gamma^{-1} (1 + R'(\bar{K}_{\text{out}}^{-1})) ,$$

where we have neglected relative corrections of the order  $R''(x) \equiv x \partial_x R'(x) = \mathcal{O}(\alpha_s)$  and assumed that  $\mathcal{F}$  is a smooth function of  $R'$  which is true for  $\mathcal{F}_\delta^R(\bar{\nu})$  in (3.16),  $d \ln \mathcal{F} / d\eta = \mathcal{O}(1)$ .

Applying these relations to our distribution in (3.16) we derive the final answer to SL accuracy,

$$\Sigma_\delta^R(K_{\text{out}}) = e^{-\mathcal{R}_\delta^R(\bar{K}_{\text{out}}^{-1})} \cdot \frac{\mathcal{F}_\delta^R(\bar{K}_{\text{out}}^{-1})}{\Gamma(1 + C_\delta r'(\bar{K}_{\text{out}}^{-1}))} , \quad \bar{K}_{\text{out}} = e^{-\gamma_E} K_{\text{out}} . \quad (3.17)$$

The first and second factors resum DL and SL contributions, respectively. We remark that the precise argument  $\bar{K}_{\text{out}}$  is essential to keep in the first factor, while substituting  $\bar{K}_{\text{out}}$  by, say,  $K_{\text{out}}$  in the second factor would amount to a negligible  $\mathcal{O}(\alpha_s)$  correction. Comparing the  $\nu$ -integrand in (3.16) with the final result we conclude that the SL factor  $\Gamma^{-1}$  in (3.17) accounts for a mismatch between the Mellin-conjugated  $\nu$  and  $K_{\text{out}}$  values. It can be looked upon as a next-to-leading order prefactor of the WKB (steepest descent) approximation.

## 4. Total $K_{\text{out}}$ -distribution

The calculation is similar to the previous case except that now radiation in all four quadrants contributes to  $K_{\text{out}}$ . The  $K_{\text{out}}$ -integrated distribution (2.9) for small  $K_{\text{out}}$  is given by

$$\begin{aligned} \frac{d\sigma(K_{\text{out}})}{dT dT_M} &= \sum_{C_\delta} \frac{d\sigma_\delta^{(0)}}{dT dT_M} \cdot \Sigma_\delta^T(K_{\text{out}}) , \\ \Sigma_\delta^T(K_{\text{out}}) &= \int \sum_n \frac{1}{n!} \prod_i^n [dk_i] W_\delta(k_i) \cdot H^T(K_{\text{out}}) , \\ H^T(K_{\text{out}}) &\equiv \int dh_n \vartheta \left( K_{\text{out}} - \sum_{a=1}^3 |q_{ax}| - \sum_i |k_{ix}| \right) . \end{aligned} \quad (4.1)$$

To factorize the soft momenta in  $H^T$  we proceed as before by using Mellin and Fourier representation for the theta- and delta-functions. Again we denote by  $\nu$  the variable conjugate to  $K_{\text{out}}$  and study the region  $|\nu|Q \gg 1$ . We rescale by  $\nu$  the variables conjugate to the soft recoil variables  $q_{ax}$  ( $a = 1, 2, 3$ ) and  $q_{1y}$  in  $dh_n$  to arrive at

$$\begin{aligned} \int dh_n \prod_{a=1}^3 e^{-\nu|q_{ax}|} \prod_{i=1}^n e^{-\nu|k_{ix}|} &= \\ \int_{-\infty}^{\infty} \frac{d\gamma}{2\pi} \left( \prod_{a=1}^3 \frac{d\beta_a}{\pi} \right) I(\beta, \gamma) &\left\{ \prod_{C_1} u_{12}(k_i) \prod_{C_4} u_{13}(k_i) \prod_{C_2} u_2(k_i) \prod_{C_3} u_3(k_i) \right\} . \end{aligned} \quad (4.2)$$

Here we have introduced the probing functions  $u_\alpha(k)$  for each of the quadrants  $C_\ell$ :

$$u_{12}(k) = u(\beta_{12}, \gamma), \quad u_{13}(k) = u(\beta_{13}, -\gamma), \quad u_2(k) = u(\beta_2, 0), \quad u_3(k) = u(\beta_3, 0), \quad (4.3)$$

where  $\beta_{12} = \beta_1 + \beta_2$ ,  $\beta_{13} = \beta_1 + \beta_3$  and the “source function”  $u$  is

$$u(\beta, \gamma) \equiv \exp \{ -\nu (|k_{ix}| + i\beta k_{ix} + i\gamma |k_{iy}|) \}. \quad (4.4)$$

The function  $I(\beta, \gamma)$  in (4.2) is the result of integrations over the recoil momenta, namely,  $q_{1y}$  (conjugate to  $\gamma$ ) and three  $q_{ax}$  (conjugate to  $\beta_a$ ):

$$I(\beta, \gamma) = \frac{1}{1 + \beta_2^2} \frac{1}{1 + \beta_3^2} \left( \frac{1}{1 + \beta_{12}^2} \frac{1}{-i\gamma + \epsilon} + \frac{1}{1 + \beta_{13}^2} \frac{1}{i\gamma + \epsilon} \right). \quad (4.5)$$

Notice that the large variable  $\nu$  enters only in the sources.

Now we are in a position to resum multiple accompanying radiation. The result reads

$$\Sigma_\delta(K_{\text{out}}) = \int \frac{d\nu}{2\pi i\nu} e^{\nu K_{\text{out}}} \int \frac{d\gamma}{2\pi} \prod_{a=1}^3 \frac{d\beta_a}{\pi} I(\beta, \gamma) \cdot e^{-\mathcal{R}_\delta(\nu, \beta, \gamma)}, \quad (4.6)$$

with the radiator given by

$$\mathcal{R}_\delta(\nu, \beta, \gamma) = \int [dk] W_\delta(k) \left[ 1 - \sum_{\ell=1}^4 u_\ell(k) \Theta_\ell(k) \right]. \quad (4.7)$$

As before, the unity in the square brackets has been included to account for the virtual correction contribution. Here  $\Theta_\ell(k)$  is the support function for a parton  $k$  emitted in the quadrant  $C_\ell$ , and we have denoted  $u_1 = u_{12}$  and  $u_4 = u_{13}$ .

In Appendix B the radiators  $\mathcal{R}_\delta$  are evaluated with SL accuracy and we obtain

$$\mathcal{R}_\delta = C_2^{(\delta)} r(\bar{\mu}_2, Q_2^2) + C_3^{(\delta)} r(\bar{\mu}_3, Q_3^2) + \frac{C_1^{(\delta)}}{\pi} \int_0^\infty \frac{dy}{1+y^2} [r(\bar{\mu}_{12}, Q_1^2) + r(\bar{\mu}_{13}, Q_1^2)], \quad (4.8)$$

where  $r$  is the DL function defined in (3.12). Some comments on the colour charges, the scales and the various  $\bar{\mu}$ -variables are in order.

- The radiator consists of three “independent” contributions from the radiation off each of three hard partons. Here

$$C_a^{(a)} = N_c; \quad C_a^{(b)} = C_F, \quad \text{for } a \neq b, \quad (4.9)$$

is the colour charge of the parton  $P_a$ .

- The hardness scale  $Q_a^2$  in each term has a simple structure: it is determined by the invariant transverse momentum of the hard parton  $a$  with respect to the dipole  $bc$ :

$$Q_a^2 = \frac{p_{ta}^2}{4} e^{-g_a}, \quad p_{ta}^2 = 2 \frac{(P_b P_a)(P_a P_c)}{(P_b P_c)}. \quad (4.10)$$

This makes  $Q_a$  depending on the event geometry. The scale  $Q_a^2$  also includes an additional, geometry-independent, factor  $e^{-g_a}$  depending on the nature of the parton  $a$ . This factor takes into account a SL correction due to hard parton splitting, with  $g_a = 3/2$  for a quark ( $a = 1, 2$  in (4.8)) and  $g_a = \beta_0/2N_c$  for a gluon. Due to this factor the scales depend on the configuration  $\delta$ .

Recall that the derivation of the exact form of the hard scales required a SL analysis which takes a due care of the inter-jet regions where the soft distribution does not have collinear singularities.

As we have seen in the previous section, the hard scales for the right distribution (3.14) do not have such a simple interpretation because selecting one hemisphere is unnatural for the soft radiation pattern. As shown in Appendices B.2.1 and B.2.2, the boundary effects due to radiation at  $90^\circ$  which complicate the scales, cancel with SL accuracy in the *total* distribution.

- The various functions  $\bar{\mu}$  originate from the following substitutions in the integral over  $k_x$

$$1 - u_a \rightarrow \vartheta(k_x - 1/\bar{\mu}_a), \quad \bar{\mu}_a = \bar{\nu} \sqrt{1 + \beta_a^2} \equiv \bar{\nu} \cdot \mu_a, \quad a = 2, 3 \quad (4.11)$$

$$1 - u_{12} \rightarrow \vartheta(k_x - 1/\bar{\mu}_{12}), \quad \bar{\mu}_{12} = \bar{\nu} \sqrt{(1 - i\gamma y)^2 + \beta_{12}^2} \equiv \bar{\nu} \cdot \mu_{12}. \quad (4.12)$$

$$1 - u_{13} \rightarrow \vartheta(k_x - 1/\bar{\mu}_{13}), \quad \bar{\mu}_{13} = \bar{\nu} \sqrt{(1 + i\gamma y)^2 + \beta_{13}^2} \equiv \bar{\nu} \cdot \mu_{13}, \quad (4.13)$$

with  $\bar{\nu}$  given in (3.11). As in the case of the right radiator, such substitution is valid within SL accuracy. The  $\gamma$ -dependence enters only in the two  $\bar{\mu}_{1a}$  parameters which are associated with the gluon emission off the parton  $P_1$  in the right hemisphere. This is in agreement with the fact that the variable  $\gamma$  is conjugate to  $q_{1y}$ . Opposite signs of  $\gamma$  in  $\bar{\mu}_{12}$  and  $\bar{\mu}_{13}$  reflect the fact that the recoil momentum  $q_{1y}$  is positive (negative) in the right-up (right-down) quadrant.

All  $\nu$ -,  $\beta$ - and  $\gamma$ -dependence is contained in the parameters  $\bar{\mu}$ .

As before, we can simplify the  $\beta$ - and  $\gamma$ -dependence by expanding the various terms to SL accuracy for large  $\nu$ . We can write

$$\mathcal{R}_\delta = R_\delta(\bar{\nu}) + r'(\bar{\nu}) \cdot S_\delta(\beta, \gamma), \quad (4.14)$$

where  $R_\delta$  is the DL contribution, given by the sum of three standard antenna terms,  $r'$  is the SL function defined in (3.15), and the coefficient  $S_\delta$  carries all the  $\beta_a$  and  $\gamma$  dependence.  $R_\delta$  and  $S_\delta$  are given by

$$\begin{aligned} R_\delta(\bar{\nu}) &= C_1^{(\delta)} r(\bar{\nu}, Q_1^2) + C_2^{(\delta)} r(\bar{\nu}, Q_2^2) + C_3^{(\delta)} r(\bar{\nu}, Q_3^2), \\ S_\delta(\beta, \gamma) &= C_2^{(\delta)} \ln \mu_2 + C_3^{(\delta)} \ln \mu_3 + \frac{C_1^{(\delta)}}{\pi} \int_0^\infty \frac{dy}{1+y^2} \ln [\mu_{12}(y) \mu_{13}(y)], \end{aligned} \quad (4.15)$$

with the charges given in (4.9). In detail the DL terms for the three configurations are

$$R_3(\bar{\nu}) = C_F r(\bar{\nu}, Q_1^2) + C_F r(\bar{\nu}, Q_2^2) + N_c r(\bar{\nu}, Q_3^2), \quad (4.16)$$

$$R_2(\bar{\nu}) = C_F r(\bar{\nu}, Q_1^2) + N_c r(\bar{\nu}, Q_2^2) + C_F r(\bar{\nu}, Q_3^2), \quad (4.17)$$

$$R_1(\bar{\nu}) = N_c r(\bar{\nu}, Q_1^2) + C_F r(\bar{\nu}, Q_2^2) + C_F r(\bar{\nu}, Q_3^2). \quad (4.18)$$

There are two sources of SL corrections in (4.14). The first is due to different hard scales in three terms  $r(\bar{\nu}, Q_1)$  in (4.16)–(4.18), which depend on the geometry of the three-jet event, that is on the values of  $T$  and  $T_M$ . The second is the contribution proportional to  $r'$  given by the sum of  $\ln \mu$ -terms which depend on  $\beta_a$  and  $\gamma$ . These contributions are specific for a three-jet topology. At the same time, within the SL accuracy this correction is insensitive to the details of the event geometry, that is to the values of  $T, T_M \sim 1$ .

In conclusion, the total  $K_{\text{out}}$ -distribution, to SL accuracy, can be expressed by the following Mellin integral:

$$\Sigma_\delta(K_{\text{out}}) = \int \frac{d\nu}{2\pi i\nu} e^{\nu K_{\text{out}}} e^{-R_\delta(\bar{\nu})} \cdot \mathcal{F}_\delta(\bar{\nu}),$$

where the SL prefactor  $\mathcal{F}_\delta(\bar{\nu})$  is given by

$$\mathcal{F}_\delta(\bar{\nu}) = \int_{-\infty}^\infty \frac{d\gamma}{2\pi} \prod_{a=1}^3 \int_{-\infty}^\infty \frac{d\beta_a}{\pi} \cdot I(\beta, \gamma) e^{-r'(\bar{\nu}) S_\delta(\beta, \gamma)}. \quad (4.19)$$

For example, the explicit expression for  $\mathcal{F}_3$  reads

$$\begin{aligned} \mathcal{F}_3(\bar{\nu}) &= \int \frac{d\gamma}{2\pi} \prod_{a=1}^3 \frac{d\beta_a}{\pi} \cdot I(\beta, \gamma) (1 + \beta_2^2)^{-\frac{1}{2} C_F r'(\bar{\nu})} (1 + \beta_3^2)^{-\frac{1}{2} N_c r'(\bar{\nu})} \\ &\quad \times \exp \left\{ -C_F r'(\bar{\nu}) \left\{ \frac{1}{\pi} \int_0^\infty \frac{dy}{1+y^2} \ln [\mu_{12}(y) \mu_{13}(y)] \right\} \right\}. \end{aligned}$$

The function  $\mathcal{F}_\delta$  is analysed in Appendix C.

In the first order in  $\alpha_s \ln \nu$  the factors  $\mathcal{F}$  become (see Appendix C.1)

$$\mathcal{F}_\delta = 1 - (3C_F + N_c) \ln 2 \cdot r'(\bar{\nu}), \quad \delta = 2, 3,$$

$$\mathcal{F}_1 = 1 - (2C_F + 2N_c) \ln 2 \cdot r'(\bar{\nu}).$$

Different weights of the quark and gluon colour factors for the two cases have a simple explanation. Due to the kinematics of parton recoil (see (2.17)) contribution of the gluon radiation off the most energetic (right-hemisphere) parton  $P_1$  is *twice* that off the left-hemisphere partons  $P_2$  and  $P_3$ . As a result, the SL correction is proportional to  $2C_F + C_F + N_c$  when  $P_1$  is a quark/antiquark ( $\delta = 2, 3$ ) and to  $2N_c + C_F + C_F$  when it is a gluon ( $\delta = 1$ ).

Integration over the Mellin variable  $\nu$  can be done as before and we obtain

$$\Sigma_\delta(K_{\text{out}}) \simeq e^{-R_\delta(\bar{K}_{\text{out}}^{-1})} \cdot \frac{\mathcal{F}_\delta(\bar{K}_{\text{out}}^{-1})}{\Gamma(1 + R'(\bar{K}_{\text{out}}^{-1}))}, \quad \bar{K}_{\text{out}} \equiv e^{-\gamma_E} K_{\text{out}}, \quad (4.20)$$

where  $R'$  is the logarithmic derivative of  $R_\delta$ . To SL accuracy we can take

$$R'(\bar{K}_{\text{out}}^{-1}) = (2C_F + N_c) \cdot r'(\bar{K}_{\text{out}}^{-1}), \quad (4.21)$$

which is the same function for all configurations  $\delta$ . This is possible since,  $r'$  being a SL function, the difference between the hard scales can be neglected at the level of the *next-to-next-to-leading*  $\mathcal{O}(\alpha_s)$  correction.

#### 4.1 Radiators in the quasi-2-jet limit

In the 3-jet kinematics we have been considering,  $T_M \lesssim T \lesssim 1$ , jet energies are comparable and relative angles between jets are large. In these circumstances three basic scales in (4.10) are of the same order,  $Q_1 \sim Q_2 \sim Q_3 \lesssim Q$ . Still, keeping precise scales in (4.16)–(4.18) is essential, since their deviation from the overall hardness parameter  $Q$  in the DL radiator function  $r(\bar{\nu}, Q_a^2)$  produced a SL correction  $\delta^{(1)}R \propto r'(\bar{\nu}, Q) \cdot \ln(Q_a/Q) = \mathcal{O}(\alpha_s \log \nu)$ . At the same time, since the next order expansion terms are negligible,  $\delta^{(2)}R \propto r''(\bar{\nu}, Q) \cdot \ln^2(Q_a/Q) = \mathcal{O}(\alpha_s)$ , it is perfectly legitimate to present the answer in a form different from (4.16)–(4.18).

For example, expanding the scales in the first two (quark) terms in  $R_3$  around  $q^2 = 2P_1P_2$  we obtain, instead of (4.16)

$$R_3 \simeq 2C_F r\left(\frac{P_1P_2}{2} e^{-\frac{3}{2}}\right) + N_c r(Q_3^2), \quad Q_3^2 = \frac{2(P_1P_3)(P_2P_3)}{(P_1P_2)} e^{-\frac{\beta_0}{2N_c}}, \quad (4.22)$$

where we have suppressed the first argument  $\bar{\nu}$  and used  $\ln \frac{p_{t1}^2}{2P_1P_2} = -\ln \frac{p_{t2}^2}{2P_1P_2}$  to cancel the linear expansion terms, see (4.10). Mismatch between the radiator in (4.16) and the right-hand side of (4.22) is

$$R_3(4.22) - R_3(4.16) = \mathcal{O}\left(\alpha_s \ln^2 \frac{P_1P_3}{P_2P_3}\right).$$

Being equivalent within the adopted accuracy, the representations (4.16) and (4.22) start to significantly differ, however, when the jet configuration becomes 2-jet-like. Indeed, when the gluon jet  $P_3$  becomes relatively soft and/or collinear to the quark

$P_2$ , we should expect the answer to correspond to the  $q\bar{q}$ -dominated radiation pattern, and the gluon contribution to disappear.

The latter representation (4.22) correctly describes this situation: the quark-antiquark antenna contribution with the hardness scale equal to the invariant squared mass of the  $q\bar{q}$  pair,  $q^2 = 2P_1P_2$ , takes on the job, while radiation off the gluon vanishes with decrease of the gluon transverse momentum,  $Q_3^2 \simeq p_{t3}^2 \ll q^2 \simeq Q^2$ . At the same time, the first representation goes hay-wire. For example, in the collinear limit,  $P_3P_2 \ll P_3P_1 \lesssim P_1P_2$ , one of the quark scales,  $Q_2^2$ , vanishes (together with  $Q_3^2$ ) while the other formally goes to infinity,  $Q_1^2 \gg Q^2$ . The geometric mean of the quark scales,  $2P_1P_2 = \sqrt{p_{1t}^2 p_{2t}^2}$ , employed in (4.22) cures this unphysical behaviour.

For two other jet configurations, with the gluon having an intermediate or the largest of the three parton energies, analogous representations of the radiators read

$$R_2 \simeq 2C_F r \left( \frac{P_1P_3}{2} e^{-\frac{3}{2}} \right) + N_c r(Q_2^2), \quad Q_2^2 = \frac{2(P_1P_2)(P_2P_3)}{(P_1P_3)} e^{-\frac{\beta_0}{2N_c}}; \quad (4.23)$$

$$R_1 \simeq N_c \left[ r \left( \frac{P_1P_2}{2} e^{-\left(\frac{3}{4} + \frac{\beta_0}{4N_c}\right)} \right) + r \left( \frac{P_1P_3}{2} e^{-\left(\frac{3}{4} + \frac{\beta_0}{4N_c}\right)} \right) \right] - \frac{1}{N_c} r \left( \frac{P_2P_3}{2} e^{-\frac{3}{2}} \right) \quad (4.24)$$

These expressions, contrary to the original ones (4.17) and (4.18), survive the limit of the left-hemisphere jets becoming quasi-collinear,  $P_2P_3 \ll P_1P_3 \lesssim P_1P_2$ . Indeed, the configuration  $\delta = 2$  is then identical, colour-wise, to  $\delta = 3$ , and (4.23) is dominated by the  $q\bar{q}$  two-jet contribution, while the non-Abelian part vanishes with the gluon transverse momentum,  $Q_2^2 \simeq p_{2t}^2 \ll Q^2$ . A rare but interesting configuration  $\delta = 1$ , where the gluon  $P_1$  in the right hemisphere is balanced by a quasi-collinear  $q\bar{q}$  pair in the left hemisphere, see (4.23), corresponds to the gluon-gluon system: radiation off the *colour-octet*  $q\bar{q}$  pair is dominated by large-angle coherent bremsstrahlung proportional to the gluon charge,  $N_c$ , with the colour-suppressed  $1/N_c$  correction term vanishing in the collinear limit.

Thus, the radiators in the form of (4.16)–(4.18) are inapplicable in the quasi-two-jet kinematics. An attentive reader could have noticed that the modified expressions (4.22)–(4.23), though better behaved, cannot pretend to uniformly preserve the desired SL accuracy. Accommodating correctly SL effects due to large-angle soft bremsstrahlung, these expressions fail, however, to properly account for “hard” SL corrections in the collinear limit.

For example, the right-hand side of (4.22) for the most natural configuration  $\delta = 3$  has a perfect *soft*-gluon limit, when  $2(P_1P_2) = Q^2$  becomes the proper 2-jet scale. At the same time, when  $P_3$  remains energetic but collinear,  $E_3 \lesssim E_2$ ,  $(P_2P_3) \rightarrow 0$ , the quark-jet scale in (4.22) remains smaller than the total annihilation energy,  $2(P_1P_2) < 2(P_1 \cdot (P_2 + P_3)) = Q^2$ . The mismatch amounts to a SL correction  $\mathcal{O}(r' \cdot \ln x_2)$ .

## 5. Discussion and conclusions

In this paper we performed the all-order perturbative analysis of the out-of-plane transverse momentum distributions in three-jet  $e^+e^-$  annihilation events. We considered the total  $K_{\text{out}}$  of the event and  $K_{\text{out}}^R$  accumulated in one event-hemisphere which contains the most energetic of three jets. The perturbative expression for the integrated  $K_{\text{out}}$ -distribution in the right (one-jet) hemisphere is given in (3.12)–(3.17) and (B.35). The  $K_{\text{out}}$ -total distribution is determined by expressions (4.8)–(4.21). These answers resum all double- and single-logarithmic contributions to the exponent (the so-called “radiator”) of the distribution in the standard Mellin-Fourier parameter space. DL and SL contributions to the radiator can be formally represented, respectively, as series  $\alpha_s^n \log^{n+1}(Q/K_{\text{out}})$  and  $\alpha_s^n \log^n(Q/K_{\text{out}})$  ( $n \geq 1$ ).

Throughout the analysis, we systematically neglected next-to-next-to-leading terms in the radiator (radiator series  $\alpha_s^n \log^{n-1} \ln(Q/K_{\text{out}})$ ,  $n \geq 1$ ) as well as non-exponentiating corrections of the relative order  $\mathcal{O}(\alpha_s)$ . The latter belong to the coefficient function  $1 + c\alpha_s + \mathcal{O}(\alpha_s^2)$ . Its first coefficient,  $c$ , is analysed in [10] where the order  $\alpha_s^2$  expansion of the approximate resummed cross is compared with numerical calculation based on the exact  $\alpha_s^2$  matrix element. Matching the resummed logarithmic expressions with the exact result is necessary for justifying exponentiation of the next-to-leading SL terms  $\alpha_s \ln(Q/K_{\text{out}})$ .

Accompanying gluon radiation pattern follows the colour topology of the underlying parton antenna. The corresponding patterns were known, to SL accuracy, for two-parton —  $q\bar{q}$  and  $gg$  — sources (quark and gluon form factors, 2-jet shapes). In the present paper we presented the first such analysis for 3-parton ensembles.

The  $q\bar{q}g$ -initiated events possess a rich colour structure which determines secondary parton flows and makes them event-geometry-dependent. We have demonstrated that after taking into account SL effects due to inter-jet gluon flows, the result can be cast as a sum of quark-antiquark ( $C_F$ ) and gluon ( $N_c$ ) contributions with the proper hardness scales depending on  $T$  and  $T_M$ .

A significant dependence on event geometry is the key feature which singles out the  $K_{\text{out}}$  distribution among other  $e^+e^-$  event shape observables.

Soft gluon field components with small transverse momenta (“gluers” with  $k_t \gtrsim \Lambda_{QCD}$ ) are believed to be responsible for hadronization. This belief, known as hypothesis of the local parton-hadron duality, has been verified in a number of experimental studies of various features of multiple hadroproduction in hard processes (for review see [19]). Moreover, in recent years a new theoretical techniques have been developed for triggering and quantifying genuine confinement effects by studying gluer radiation.

A rich dependence of gluon (and, therefore, gluer) radiation on the colour topology makes 3-jet observables, and  $K_{\text{out}}$  in particular, an interesting field for the study of non-perturbative effects. A separate publication [13] will be devoted to analysis of

the leading non-perturbative power-suppressed corrections to 3-jet observables. The  $K_{\text{out}}$  distribution, similar to the case of 2-jet Broadening observables [12], will be shown to exhibit  $\log K_{\text{out}}$ -enhanced  $1/Q$  contribution with the magnitude depending on 3-jet geometry, that is on  $T$  and  $T_M$  values.

To access this interesting physics experimental studies of  $K_{\text{out}}$  should be carried out specifically for events with moderate values of  $1 - T$ , away from the 2-jet region.

Two sorts of experimental studies of these predictions can be envisaged. The most straightforward comparison calls for experimental identification of the gluon jet. Gluon tagging, however, is unnecessary for the study of the total  $K_{\text{out}}$ -distribution for genuine 3-jet events: the prediction given by the sum of three jet configurations corresponding to given  $T$  and  $T_M$ , weighted with the proper 3-jet Born cross section factors bears practically as much information. Tagging brings in more information when a single-jet (right-jet)  $K_{\text{out}}$ -distribution is studied. In this case essentially different  $K_{\text{out}}$ -spectra will be seen depending on whether the right-hemisphere parton is a quark or a gluon.

## Acknowledgements

We are grateful to Gavin Salam for helpful discussions and suggestions.

## A. Kinematics

### A.1 Kinematics of $q\bar{q}g$ jets

We consider the quark, antiquark and gluon with skeleton momenta  $P_a$  in the centre-of-mass frame,  $\sum_{a=1}^3 P_a = Q = (Q, 0, 0, 0)$ ,

$$P_1 = E(x_1, 0, 0, t_1), \quad P_2 = E(x_2, 0, T_M, -t_2), \quad P_3 = E(x_3, 0, -T_M, -t_3). \quad (\text{A.1})$$

We have  $2E = Q$ ,  $x_a = 2(P_a Q)/Q^2$ ,  $x_1 + x_2 + x_3 = 2$  and  $t_1 = t_2 + t_3$ . Assuming  $x_2 > x_3$ , we obtain

$$\begin{aligned} x_1 &= T, & t_1 &= T, \\ x_2 &= \frac{2-T}{2} + \frac{T}{2}\rho, & t_2 &= \frac{T}{2} + \frac{2-T}{2}\rho, \\ x_3 &= \frac{2-T}{2} - \frac{T}{2}\rho, & t_3 &= \frac{T}{2} - \frac{2-T}{2}\rho, \end{aligned} \quad (\text{A.2})$$

where

$$\rho \equiv \sqrt{1 - \frac{T_M^2}{1-T}} < 1. \quad (\text{A.3})$$

Thrust-major is confined to the kinematical region

$$\frac{2(1-T)}{T}\sqrt{2T-1} < T_M < \sqrt{1-T}, \quad (\text{A.4})$$

where the upper limit comes from reality of  $\rho$ , and the lower limit comes from requiring  $x_1 > x_2$ . It is straightforward to show that in this kinematical region  $t_3 > 0$ , i.e. that both  $P_2$  and  $P_3$  lie in the left hemisphere.

We introduce Sudakov variables based on two light-light vectors aligned with the thrust axis,

$$P = E(1, 0, 0, 1), \quad \bar{P} = E(1, 0, 0, -1). \quad (\text{A.5})$$

The jet momenta have the following Sudakov decomposition:

$$P_1 = TP, \quad P_2 = A_2 P + B_2 \bar{P} + P_t, \quad P_3 = A_3 P + B_3 \bar{P} - P_t, \quad (\text{A.6})$$

where the transverse momentum with respect to the thrust axis is  $P_t = (0, 0, ET_M, 0)$ . In terms of  $T$  and  $T_M$  the longitudinal Sudakov momentum components are

$$\begin{aligned} A_2 &= \frac{1-T}{2}(1-\rho), & B_2 &= \frac{1}{2}(1+\rho), \\ A_3 &= \frac{1-T}{2}(1+\rho), & B_3 &= \frac{1}{2}(1-\rho). \end{aligned} \quad (\text{A.7})$$

Since  $P_a$  with  $a = 2, 3$  belong to the left hemisphere, we have  $A_a < B_a$ .

Denoting by  $\Theta_a$  the angle of  $\vec{P}_a$  with respect to the thrust axis we introduce the angular variables  $\tau_a$

$$\begin{aligned} \frac{\tau_2}{Q} &\equiv \tan \frac{\Theta_2}{2} = \frac{P_t}{QA_2} = \frac{1+\rho}{T_M}, \\ \frac{\tau_3}{Q} &\equiv \tan \frac{\Theta_3}{2} = \frac{-P_t}{QA_3} = -\frac{1-\rho}{T_M}. \end{aligned} \quad (\text{A.8})$$

We remark that  $\tau_3$  is negative since  $P_3$  lies in the third quadrant (“down” hemisphere). Since  $P_2$  and  $P_3$  are in the left hemisphere and  $|P_{2z}| > |P_{3z}|$ , we have  $0 < \pi - \Theta_2 < \Theta_3 - \pi < \frac{1}{2}\pi$ . Hence,

$$\frac{\tau_2}{Q} > \frac{-\tau_3}{Q} > 1.$$

The following relations hold:

$$\tau_2 |\tau_3| = \frac{Q^2}{1-T}, \quad \tau_2 + |\tau_3| = \frac{2Q}{T_M}. \quad (\text{A.9})$$

The minimal value of thrust-major,  $T_M = 2(1-T)/(2-T)$  for a given  $T$  in (A.4), corresponds to the configuration with the softest parton momentum orthogonal to the thrust axis,

$$\rho \rightarrow \frac{T}{2-T}, \quad \frac{\tau_2}{Q} \rightarrow \frac{1}{1-T}, \quad \frac{|\tau_3|}{Q} \rightarrow 1.$$

The maximal value  $T_M = \sqrt{1-T}$  is achieved with a symmetric  $2--3$  pair:

$$\rho \rightarrow 0, \quad \frac{\tau_2}{Q} \rightarrow \frac{|\tau_3|}{Q} \rightarrow \frac{1}{\sqrt{1-T}}.$$

We also introduce two-dimensional vectors in the transverse plane  $\{x, y\}$ ,

$$\vec{\tau}_2 \equiv \frac{\vec{P}_t}{A_2} = (0, \tau_2), \quad \vec{\tau}_3 \equiv \frac{-\vec{P}_t}{A_3} = (0, \tau_3). \quad (\text{A.10})$$

Since  $P_1$  is along the thrust axis we have  $\vec{\tau}_1 = (0, 0)$ .

## A.2 Born cross sections

The squared Born matrix element  $M_0(\mathcal{C}_\delta)$  has a well-known expression in terms of the variables  $x_a$ . For  $\delta = 3$  (with  $P_3$  the gluon momentum) we have

$$M_0^2(\mathcal{C}_3) = \frac{C_F}{2\pi} \alpha_s(Q) \frac{x_1^2 + x_2^2}{(1-x_1)(1-x_2)}. \quad (\text{A.11})$$

The phase space factor  $\Gamma_0$  for the Born 3-parton system is

$$\Gamma_0 = \frac{1}{8(2\pi)^5} \prod_{a=1}^3 \frac{d^3 p_a}{E_a} \delta^4(Q - \sum p_a) \delta^3(\vec{p}_1 - \vec{P}_1) \delta^2(\vec{p}_{t2} - \vec{P}_{t2}) \quad (\text{A.12})$$

The dipole invariant masses in terms of  $T, T_M$  and variables  $\tau_i$  are

$$\begin{aligned} Q_{12}^2 &= 2P_1P_2 = \frac{T}{2}(1+\rho)Q^2 = \frac{1}{2}TT_M\tau_2Q, \\ Q_{13}^2 &= 2P_1P_3 = \frac{T}{2}(1-\rho)Q^2 = \frac{1}{2}TT_M|\tau_3|Q, \\ Q_{23}^2 &= 2P_2P_3 = (1-T)Q^2 = \frac{Q^4}{\tau_2|\tau_3|}. \end{aligned} \quad (\text{A.13})$$

The scales in (4.10),

$$p_{ta}^2 \equiv \frac{2(P_b P_a)(P_a P_c)}{(P_b P_c)},$$

— the invariant transverse momentum of the hard parton  $P_a$  with respect to the  $bc$ -dipole — read

$$p_{t1}^2 = \frac{Q^2}{2} \left( \frac{TT_M}{1-T} \right)^2, \quad p_{t2}^2 = Q^2(1-T) \left( \frac{1+\rho}{T_M} \right)^2, \quad p_{t3}^2 = Q^2(1-T) \left( \frac{1-\rho}{T_M} \right)^2. \quad (\text{A.14})$$

### A.3 Soft partons

For secondary massless parton of momentum  $k$  we write the Sudakov representation

$$k = \alpha P + \beta \bar{P} + k_t, \quad \alpha\beta = \frac{k_t^2}{Q^2}, \quad (\text{A.15})$$

with  $\vec{k}_t$  the transverse momentum with respect to the thrust axis. The right-hemisphere condition imposes the restriction upon longitudinal parton components,

$$\alpha > \beta \Rightarrow \alpha > \frac{k_t}{Q}.$$

Probability of soft gluon emission off the  $P_a, P_b$  dipole is described by the squared matrix element

$$\frac{P_a P_b}{2(P_a k)(k P_b)} = \frac{\alpha^2 (\vec{\tau}_a - \vec{\tau}_b)^2}{(\vec{k}_t - \alpha \vec{\tau}_a)^2 (\vec{k}_t - \alpha \vec{\tau}_b)^2}. \quad (\text{A.16})$$

## B. Radiators

Here we compute the radiators for the total  $K_{\text{out}}$  distribution,  $\mathcal{R}_\delta(\nu, \beta, \gamma)$ , to SL accuracy. The radiator is given by the combination of dipole contributions,

$$r_{ab} = \int [dk] w_{ab}(k) \sum_{\ell=1}^4 [1 - u_\ell] \Theta_\ell(k), \quad (\text{B.1})$$

with  $\Theta_\ell(k)$  the support function restricting gluon momentum  $k$  to the quadrant  $C_\ell$  and the source functions  $u_\ell$  defined in (4.3), (4.4).

Expressing the parton phase space  $[dk]$  in terms of Sudakov variables and invoking the soft distribution  $w_{ab}$  in (A.16) we have

$$r_{ab} = \int_{-Q}^Q dk_x \int_{-K_{ym}}^{K_{ym}} \frac{dk_y}{\pi} \int_0^{\alpha_m} \frac{d\alpha}{\alpha} \left\{ \frac{\alpha_s(k_{t,ab})}{\pi} \frac{\alpha^2 (\vec{\tau}_a - \vec{\tau}_b)^2}{(\vec{k}_t - \alpha \vec{\tau}_a)^2 (\vec{k}_t - \alpha \vec{\tau}_b)^2} \right\} \sum_\ell [1 - u_\ell] \Theta_\ell(k). \quad (\text{B.2})$$

We recall that  $\vec{\tau}_a$  are jet transverse direction vectors,  $\vec{\tau}_1 = 0$  and  $\vec{\tau}_{2,3}$  given in (A.10).

We have three integrations to perform. The result of the first two integrals, in  $\alpha$  and  $k_y$ , has the structure

$$\int k_y \int d\alpha \propto \frac{\alpha_s}{|k_x|} \left( \ln \frac{Q'}{|k_x|} + \mathcal{O}(k_x) \right), \quad \frac{Q'}{Q} = \mathcal{O}(1), \quad (\text{B.3})$$

where we have omitted  $\mathcal{O}(k_x)$  terms as producing non-logarithmic  $\mathcal{O}(\alpha_s)$  corrections upon  $k_x$ -integration. (For the same reason we have set the lower limit of

$\alpha$ -integration,  $\alpha \gtrsim (k_t/Q)^2$ , to zero, since the integral converges.) Similar correction originates from the precise limit of the  $k_x$  integration,  $|k_x| \lesssim Q$ . Therefore we were free to set it to  $Q$  in (B.2). <sup>2</sup>

At the same time, the exact limits of  $\alpha$  and  $k_y$  integrals do matter when they affect the scale of the logarithm,  $Q'$ , in (B.3) which are responsible for the SL correction to the radiator. The logarithmic terms in (B.3) originate from three “collinear regions” when the gluon transverse direction vector  $\vec{\tau} = \vec{k}_t/\alpha$  is close to one of  $\vec{\tau}_a$ . In the direction  $P_1$  it is the  $\alpha$ -integration that produces a collinear logarithm. Noticing that  $P_{1z} = TQ/2$ , we then set  $\alpha_m$  to the maximal value of  $\alpha$  kinematically allowed in the right-hemisphere jet,

$$\alpha_m = T. \quad (\text{B.4})$$

In the regions collinear to the left-hemisphere jets  $a = 2, 3$ ,  $\alpha$  and  $k_y$  are linked by the condition  $\vec{\tau} \simeq \vec{\tau}_a$ . In this case the kinematical limit can be expressed in terms of the  $y$ -component:  $P_{2y} = |P_{3y}| = T_M Q/2$  translates into

$$K_{ym} = \frac{T_M Q}{2}. \quad (\text{B.5})$$

In (B.2) we employed soft radiation probabilities  $w_{ab}$ . However, in the collinear regions hard parton splitting should be accounted for which produces another important SL corrections similar to those coming from the kinematical limits (B.4) and (B.5). These corrections will be taken care of in the end of Appendix B.2.2.

We now proceed with successive integrations. Since the sources  $u$  do not depend on  $\alpha$  we first compute the  $\alpha$ -integral. Then we compute the  $k_y$ - and  $k_x$ -integrals.

## B.1 Integrating over $\alpha$

We calculate separately contributions from the right ( $R$ ) and left ( $L$ ) hemispheres,

$$R \Rightarrow \frac{k_t}{Q} < \alpha < \alpha_m = T, \quad L \Rightarrow \alpha < \frac{k_t}{Q}, \quad (\text{B.6})$$

and define

$$I_{ab}^R = \int_{k_t/Q}^{\alpha_m} \frac{\alpha d\alpha (\vec{\tau}_a - \vec{\tau}_b)^2}{(\vec{k}_t - \alpha \vec{\tau}_a)^2 (\vec{k}_t - \alpha \vec{\tau}_b)^2}, \quad I_{ab}^L = \int_0^{k_t/Q} \frac{\alpha d\alpha (\vec{\tau}_a - \vec{\tau}_b)^2}{(\vec{k}_t - \alpha \vec{\tau}_a)^2 (\vec{k}_t - \alpha \vec{\tau}_b)^2}. \quad (\text{B.7})$$

The  $\alpha$ -integration yields

$$\begin{aligned} & \int_0^\alpha \frac{\alpha d\alpha (\vec{\tau}_a - \vec{\tau}_b)^2}{(\vec{k}_t - \alpha \vec{\tau}_a)^2 (\vec{k}_t - \alpha \vec{\tau}_b)^2} \\ &= \frac{1}{k_y^2 + h_{ab}^2 k_x^2} \left\{ \frac{h_{ab}}{2} \ln \frac{(\alpha \tau_a - k_y)^2 + k_x^2}{(\alpha \tau_b - k_y)^2 + k_x^2} + \frac{k_y}{|k_x|} \left( \arctan \frac{\alpha \tau_a - k_y}{|k_x|} + \arctan \frac{\alpha \tau_b - k_y}{|k_x|} \right) \right\}. \end{aligned} \quad (\text{B.8})$$

---

<sup>2</sup>We remind the reader that all these  $\mathcal{O}(\alpha_s)$  uncertainties, as well as those we shall encounter below, are related to the coefficient function [10].

Here  $h_{ab}$  is a function of  $\tau_a$  and  $\tau_b$  which has the following geometrical meaning:

$$h_{ab} = \frac{\tau_a + \tau_b}{\tau_a - \tau_b} = \frac{\tan \frac{1}{2}\theta_a + \tan \frac{1}{2}\theta_b}{\tan \frac{1}{2}\theta_a - \tan \frac{1}{2}\theta_b} = \frac{\sin \frac{1}{2}(\theta_a + \theta_b)}{\sin \frac{1}{2}(\theta_a - \theta_b)}, \quad (\text{B.9})$$

with  $\theta_a$  the angle between the momentum  $\vec{P}_a$  and the thrust axis. We have  $h_{a1} = 1$  ( $a = 2, 3$ ) and  $h_{23} = \rho$ .

In the limit of small aplanarity,  $|k_x| \ll Q$ , for the dipoles involving the right-hemisphere jet  $P_1$  we derive

$$I_{1a}^R = \frac{1}{k_t^2} \left\{ \frac{1}{2} \ln \frac{\alpha_m^2 \tau_a^2}{\kappa_a^2 + k_x^2} + \frac{k_y}{|k_x|} \left( \frac{\pi}{2} (1 - 2\vartheta(-\tau_a)) - \arctan \frac{\kappa_a}{|k_x|} \right) \right\}, \quad (\text{B.10})$$

$$I_{1a}^L = \frac{1}{k_t^2} \left\{ \frac{1}{2} \ln \frac{\kappa_a^2 + k_x^2}{k_t^2} + \frac{k_y}{|k_x|} \left( \arctan \frac{\kappa_a}{|k_x|} + \arctan \frac{k_y}{|k_x|} \right) \right\}. \quad (\text{B.11})$$

For the left-hemisphere dipole we get

$$\begin{aligned} I_{23}^R &= \frac{1}{k_y^2 + \rho^2 k_x^2} \cdot \left\{ \frac{\rho}{2} \ln \frac{\tau_2^2}{\tau_3^2} + \frac{\rho}{2} \ln \frac{\kappa_3^2 + k_x^2}{\kappa_2^2 + k_x^2} - \frac{k_y}{|k_x|} \left( \arctan \frac{\kappa_2}{|k_x|} + \arctan \frac{\kappa_3}{|k_x|} \right) \right\}, \\ I_{23}^L &= \frac{1}{k_y^2 + \rho^2 k_x^2} \cdot \left\{ \frac{\rho}{2} \ln \frac{\kappa_2^2 + k_x^2}{\kappa_3^2 + k_x^2} \right. \\ &\quad \left. + \frac{k_y}{|k_x|} \left( \arctan \frac{\kappa_2}{|k_x|} + \arctan \frac{\kappa_3}{|k_x|} + 2 \arctan \frac{k_y}{|k_x|} \right) \right\}. \end{aligned} \quad (\text{B.12})$$

Here

$$\kappa_a \equiv \frac{k_t}{Q} \tau_a - k_y, \quad \kappa_2 > 0, \quad \kappa_3 < 0.$$

## B.2 Integrating over $k_y$

To obtain the  $k_x$ -integrand we need to perform the  $k_y$ -integration

$$r_{ab} = \int_{-Q}^Q dk_x \frac{\alpha_s(2|k_x|)}{\pi} B_{ab}(k_x). \quad (\text{B.13})$$

The origin of the running coupling argument in (B.13) is explained below in Appendix B.5.

To compute the functions  $B_{ab}(k_x)$  we consider two terms  $B_{ab}^{(U)}$  and  $B_{ab}^{(D)}$  coming from the upper ( $U$ ) and lower ( $D$ ) hemispheres, each containing left- and right-hemisphere contributions,

$$B_{ab}^{(U)} = \int_0^{K_{ym}} \frac{dk_y}{\pi} \left\{ I_{ab}^L \cdot [1 - u_2] + I_{ab}^R \cdot [1 - u_{12}] \right\}, \quad (\text{B.14})$$

and

$$B_{ab}^{(D)} = \int_{-K_{ym}}^0 \frac{dk_y}{\pi} \left\{ I_{ab}^L \cdot [1 - u_3] + I_{ab}^R \cdot [1 - u_{13}] \right\}. \quad (\text{B.15})$$

From (4.3) we have

$$u_{12} = u(\beta_{12}, \gamma), \quad u_{13} = u(\beta_{13}, -\gamma), \quad u_2 = u(\beta_2, 0), \quad u_3 = u(\beta_3, 0), \quad (\text{B.16})$$

where  $\beta_{1a} = \beta_1 + \beta_a$  and

$$u(\beta, \gamma) = e^{-\nu[|k_x| + i\beta k_x + i\gamma|k_y|]}. \quad (\text{B.17})$$

Only the right-hemisphere sources  $u_{1a}$  depend on  $k_y$ .

### B.2.1 Dipole 23

Consider first the 23-dipole contributions  $B_{23}^{(U/D)}$ . The DL piece is obviously contained in the left-hemisphere piece  $I_{23}^L$ . At the same time, the contributions involving  $I_{23}^R$  are subleading: their  $k_y$ -integrals are not enhanced by  $\log |k_x|$ . Therefore, with SL accuracy the accompanying  $[1 - u_{1a}]$  factors in (B.14) and (B.15) can be simplified, set equal to  $[1 - u_a]$  and factored out:

$$I_{23}^L \cdot [1 - u_a] + I_{23}^R \cdot [1 - u_{1a}] \rightarrow (I_{23}^L + I_{23}^R) \cdot [1 - u_a].$$

Then, the terms in  $I_{23}^R$  and  $I_{23}^L$  due to the boundary between the  $R$ - and  $L$ -hemispheres cancel in the sum, and, using that the sources are now  $k_y$ -independent, we obtain

$$\begin{aligned} B_{23}^{(U)} &= [1 - u_2] \cdot \mathcal{L}, & B_{23}^{(D)} &= [1 - u_3] \cdot \mathcal{L}; \\ \mathcal{L} &= \int_0^{K_{ym}} \frac{dk}{\pi(k^2 + \rho^2 k_x^2)} \left( \frac{\rho}{2} \ln \frac{\tau_2^2}{\tau_3^2} + \frac{2k}{|k_x|} \arctan \frac{k}{|k_x|} \right), \end{aligned} \quad (\text{B.18})$$

where  $k = k_y$  ( $k = -k_y$ ) in the up (down) hemisphere. We extract the logarithmic contribution coming from the arctan term in the region  $|k_x| \ll k \ll K_m = \frac{1}{2}T_M Q$  (see (B.5)) and using

$$\int_0^\infty \frac{2k dk}{\pi(k^2 + \rho^2 k_x^2)} \arctan \frac{|k_x|}{k} = \ln \frac{1 + \rho}{\rho}, \quad (\text{B.19})$$

we finally arrive at

$$\mathcal{L} = \frac{1}{2} \ln \frac{(1 - T)Q^2}{4k_x^2}, \quad (\text{B.20})$$

where we have used the relations

$$T_M^2 = (1 - T)(1 - \rho^2) \quad \text{and} \quad \frac{\tau_2}{|\tau_3|} = \frac{1 + \rho}{1 - \rho},$$

following from (A.3) and (A.8), respectively.

### B.2.2 Dipoles 12 and 13

The contributions 1a can be simplified in a similar way. The left-hemisphere contribution (B.11) is accompanied by  $k_y$ -independent source  $u_a$ . The same source can be attributed, however, to the second term in (B.10) as well, since the  $k_y$ -integration is non-logarithmic and produces a subleading contribution. After this simplification the  $R/L$ -boundary terms cancel in the sum of  $I_{1a}^R$  and  $I_{1a}^L$ , and we arrive at

$$B_{1a}^{(U)} = \int_0^{K_{ym}} \frac{dk_y}{\pi k_t^2} \left( \frac{1}{2} \ln \frac{\alpha_m^2 \tau_a^2}{k_t^2} [1 - u_{12}] + \frac{k_y}{|k_x|} \left[ \frac{\pi}{2} \operatorname{sgn}(\tau_a) + \arctan \frac{k_y}{|k_x|} \right] [1 - u_2] \right) \quad (B.21)$$

$$B_{1a}^{(D)} = \int_{-K_{ym}}^0 \frac{dk_y}{\pi k_t^2} \left( \frac{1}{2} \ln \frac{\alpha_m^2 \tau_a^2}{k_t^2} [1 - u_{13}] + \frac{k_y}{|k_x|} \left[ \frac{\pi}{2} \operatorname{sgn}(\tau_a) + \arctan \frac{k_y}{|k_x|} \right] [1 - u_3] \right) \quad (B.22)$$

As before, it is important to keep the dependence of the sources on the finite parameters  $\beta$  and  $\gamma$  only in the contributions enhanced by  $\ln(Q/|k_x|)$ . Such factor (collinear logarithm due to the jet #1) is explicitly present in the first terms in (B.21), (B.22). Adding these contributions together and integrating over  $k_y$  results in substituting the R-hemisphere sources by the average source,

$$\frac{[1 - \bar{u}_1]}{2|k_x|} \ln \frac{Q^2}{k_x^2},$$

where

$$1 - \bar{u}_1 \equiv \frac{1}{\pi} \int_0^\infty \frac{dy}{1 + y^2} [(1 - u_{12}) + (1 - u_{13})], \quad y \equiv |k_y/k_x|.$$

Collinear enhancement factor due to the jet #2 originates from logarithmic  $k_y$ -integration in the second term of (B.21) (second quadrant), due to the jet #3 — in the second term of (B.22) (third quadrant). Remaining finite pieces can be evaluated using (B.19).

Setting the limits  $\alpha_m = T$  and  $K_{ym} = T_M Q/2$  according to (B.4) and (B.5) and using (A.8), we finally obtain

$$B_{1a} = B_{1a}^{(U+D)} = \frac{(1 - \bar{u}_1)}{2|k_x|} \ln \frac{Q^2}{k_x^2} + \frac{(1 - u_a)}{2|k_x|} \ln \frac{Q^2}{k_x^2} + \frac{(1 - u_0)}{|k_x|} \ln \frac{TT_M|\tau_a|}{8Q}, \quad (B.23)$$

where  $u_0$  in the last subleading term is a source whose  $\beta$ -,  $\gamma$ -dependence can be chosen arbitrary. Using this freedom we can absorb the last term in (B.23) into rescaling of the first two namely,

$$\ln \frac{Q^2}{k_x^2} \rightarrow \ln \frac{TT_M|\tau_a|Q}{8k_x^2}. \quad (B.24)$$

We observe that the hard scales in (B.20) and (B.24) have a simple geometrical interpretation. Indeed,

$$(1 - T)Q^2 = 2P_2P_3 = Q_{23}^2, \quad \frac{TT_M|\tau_a|Q}{2} = 2P_1P_a = Q_{1a}^2, \quad (B.25)$$

with  $Q_{ab}$  the invariant dipole masses, see (A.13).

Our analysis was based up to now on the soft radiation matrix element, (A.16). To fully take into account SL effects from the region of large secondary parton momenta, we have, in addition to fixing the upper limits  $\alpha_m$  and  $k_{ym}$ , to consider also hard collinear parton splitting. Due to collinear factorization, these corrections are process-independent and can be easily taken into account by proper rescaling of jet hardness parameters. They amount to supplying the invariant dipole masses by the factors

$$Q_{ab}^2 \rightarrow Q_{ab}^2 \cdot \exp \left\{ -\frac{1}{2}(g_a + g_b) \right\}, \quad g_a = \begin{cases} \frac{3}{2} & \text{for a quark/antiquark,} \\ \frac{\beta_0}{2N_c} & \text{for a gluon.} \end{cases} \quad (\text{B.26})$$

We finally obtain

$$\begin{aligned} B_{23} &= \frac{[(1 - u_2) + (1 - u_3)]}{2 |k_x|} \ln \frac{Q_{23}^2 e^{-\frac{1}{2}(g_2 + g_3)}}{4k_x^2}, \\ B_{1a} &= \frac{[(1 - \bar{u}_1) + (1 - u_a)]}{2 |k_x|} \ln \frac{Q_{1a}^2 e^{-\frac{1}{2}(g_1 + g_a)}}{4k_x^2}. \end{aligned} \quad (\text{B.27})$$

### B.3 Radiator by assembling bits and pieces

Now that the  $\alpha$ - and  $k_y$ -integrations have been performed, we are in a position to assemble the full radiators for three jet configurations:

$$\mathcal{R}_3 = \int_{-Q}^Q dk_x \frac{\alpha_s(2|k_x|)}{\pi} \frac{N_c}{2} \left( B_{13} + B_{23} - \frac{1}{N_c^2} B_{12} \right), \quad (\text{B.28})$$

$$\mathcal{R}_2 = \int_{-Q}^Q dk_x \frac{\alpha_s(2|k_x|)}{\pi} \frac{N_c}{2} \left( B_{12} + B_{23} - \frac{1}{N_c^2} B_{13} \right), \quad (\text{B.29})$$

$$\mathcal{R}_1 = \int_{-Q}^Q dk_x \frac{\alpha_s(2|k_x|)}{\pi} \frac{N_c}{2} \left( B_{12} + B_{13} - \frac{1}{N_c^2} B_{23} \right). \quad (\text{B.30})$$

The answers assume a simple when expressed in terms of the invariant transverse momentum of the hard parton  $P_a$  with respect to the  $bc$ -dipole

$$p_{ta}^2 \equiv \frac{Q_{ba}^2 Q_{ac}^2}{Q_{bc}^2}.$$

It is straightforward to verify that, to SL accuracy, the answer can be represented in a symmetric form as

$$\mathcal{R}_\delta = \int_{-Q}^Q \frac{dk_x \alpha_s(2|k_x|)}{k_x 2\pi} \left( C_1^{(\delta)} \ln \frac{Q_1^2}{k_x^2} [1 - \bar{u}_1] + C_2^{(\delta)} \ln \frac{Q_2^2}{k_x^2} [1 - u_2] + C_3^{(\delta)} \ln \frac{Q_3^2}{k_x^2} [1 - u_3] \right), \quad (\text{B.31})$$

where the hard scales are given by:

$$Q_1^2 = \frac{p_{t1}^2}{4} e^{-g_1}, \quad Q_2^2 = \frac{p_{t2}^2}{4} e^{-g_2}, \quad Q_3^2 = \frac{p_{t3}^2}{4} e^{-g_3}. \quad (\text{B.32})$$

The rule for the colour factors in (B.31) is simple:

$$C_a^{(a)} = N_c; \quad C_b^{(a)} = C_F, \quad \text{for } a \neq b, \quad (\text{B.33})$$

and the hard-splitting rescaling factors  $e^{-g_a}$  are defined in (B.26).

The universal representations (B.28)–(B.30) do not have a smooth 2-jet limit. In subsection 4.1 alternative formulae are presented which are equivalent to the previous ones in the 3-jet kinematics,  $T_M \lesssim T = \mathcal{O}(1)$ , but are better behaved when the system assumes a quasi-two-jet kinematics,  $T_M \ll T$ .

#### B.4 Radiator for the right distribution

In this case the source does not depend on  $k_y$ , and we have

$$\begin{aligned} \mathcal{R}_{ab}^R(\nu, \beta) &= \int_{-Q}^Q dk_x \frac{\alpha_s(2|k_x|)}{\pi} B_{ab}^R(k_x), \\ B_{ab}^R(k_x) &= [1 - e^{-\nu(|k_x| + i\beta k_x)}] \cdot \int_{-\infty}^{\infty} \frac{dk_y}{\pi} I_{ab}^R, \end{aligned} \quad (\text{B.34})$$

where the functions  $I_{ab}^R$  are given in (B.10) and (B.12). The DL contribution is contained in the first term of  $I_{1a}^R$  in (B.10). Extracting the large logarithm  $\ln(Q^2/k_x)$  which is embodied into the DL function  $r(\bar{\mu}, Q^2)$  in (3.9), we calculate the geometry-dependent SL correction factors denoted there by  $F_{ab}$ .

The  $k_y$  integrals are convergent so we have set the upper limit  $K_{ym} \rightarrow \infty$ . Introducing the ratio of momenta  $t = k_y / |k_x|$  we obtain the following expressions:

$$\begin{aligned} F_{1a}(\tau_a) &= 2 \ln \frac{\alpha_m |\tau_a|}{Q} + 2 \int_{-\infty}^{\infty} \frac{dt}{\pi(1+t^2)} \left\{ -\frac{1}{2} \ln \left( 1 + \kappa_a'^2 \right) \right. \\ &\quad \left. + t \left( \frac{\pi}{2} \operatorname{sgn}(\tau_a) - \arctan(\kappa_a') \right) \right\}, \\ F_{23}(\tau_2, \tau_3) &= 2 \ln \frac{\tau_2}{|\tau_3|} + 2 \int_{-\infty}^{\infty} \frac{dt}{\pi(\rho^2 + t^2)} \left\{ \frac{\rho}{2} \ln \left( \frac{1 + \kappa_3'^2}{1 + \kappa_2'^2} \right) \right. \\ &\quad \left. - t (\arctan(\kappa_2') + \arctan(\kappa_3')) \right\}. \end{aligned} \quad (\text{B.35})$$

where  $\kappa_a' \equiv \frac{\kappa_a}{|k_x|} = \sqrt{1 + t^2 \frac{\tau_a}{Q}} - t$ . We remind the reader that convergence of the integrals is assured by  $\tau_2 > 1$ ,  $\tau_3 < -1$ .

## B.5 Running coupling

The two-loop analysis [15] entails that the argument of the running coupling for the dipole distribution  $r_{ab}$  in (B.1) is given by  $k_{t,ab}$ , the invariant gluon transverse momentum with respect to the  $ab$ -dipole (see(2.24)). We show here that, to SL accuracy, we can the scale at the value  $2|k_x|$  instead, as has been stated in (B.13). This effective value is obtained after integrating  $\alpha_s(k_{t,ab})$  over  $\alpha$  and  $k_y$ . To show this we first observe that we need to control the precise argument of  $\alpha_s$  only in the DL contributions which originate from the phase space regions where the gluon is collinear to one of the three hard partons  $P_a$ .

Consider first the case of the contribution of  $r_{1a}$  from the right hemisphere. Here the soft gluon is close to the thrust axis,  $P_1$ , so that the invariant transverse momentum reduces to the usual 2-dimensional momentum,  $k_{t,1a}^2 \simeq k_t^2 = k_x^2 + k_y^2$ , which is  $\alpha$ -independent. This allows us to perform the  $\alpha$ -integration and obtain  $I_{1a}^R$  in (B.10).

Now, to determine the effective scale of  $\alpha_s$  it suffices to consider  $k_y$ -integral of the leading piece of  $I_{1a}^R$  proportional to  $\ln(Q^2/k_x^2)$  and integrate over  $k_y$ . We have an integral of the type

$$A = \int_{-K_{ym}}^{K_{ym}} \frac{dk_y}{\pi k_t^2} \alpha_s(k_t) = \frac{1}{k_x} \int_{-y_m}^{y_m} \frac{dy}{\pi(1+y^2)} \alpha_s(k_x \sqrt{1+y^2}) , \quad (\text{B.36})$$

with  $k_x$  positive,  $y \equiv k_y/k_x$ . For small  $k_x$  the upper limit of the  $y$ -integral is large,  $y_m = K_{ym}/k_x = T_M Q/2k_x \gg 1$ , and can set infinite since the integral converges. Expanding the coupling to the first order, we get

$$\begin{aligned} k_x \cdot A &= \int_{-\infty}^{\infty} \frac{dy}{\pi(1+y^2)} \left( \alpha_s(k_x) - \frac{\beta_0}{4\pi} \alpha_s^2(k_x) \ln(1+y^2) \right) + \mathcal{O}(\alpha_s^3) \\ &\simeq \left( \alpha_s(k_x) - \frac{\beta_0}{4\pi} \alpha_s^2(k_x) \ln 4 \right) \simeq \alpha_s(2k_x) . \end{aligned} \quad (\text{B.37})$$

The regions collinear to  $P_2$  or  $P_3$  seems more complicated since here  $k_{t,ab}$  depend both on  $\alpha$  and  $k_y$ . However, a similar analysis can be carried out in terms of the Sudakov variables with  $P, \bar{P}$  aligned with the emitting parton, we obtain the same result for the argument of  $\alpha_s$ .

## B.6 The sources and the $k_x$ integrals

Here we prove the substitution rule (4.11). The general structure of the radiators is

$$D = \int_0^Q \frac{dk_x}{k_x} \ln \frac{Q'}{k_x} [1 - u] , \quad u \equiv e^{-\nu k_x} \cos(\nu \beta k_x) e^{i \nu \gamma y k_x} , \quad (\text{B.38})$$

with  $Q' = \mathcal{O}(Q)$  a hard scale. This we write as

$$D = \int_{1/\bar{\mu}}^Q \frac{dk_x}{k_x} \ln \frac{Q'}{k_x} + \Delta, \quad \Delta = \frac{-\partial}{\partial \epsilon} \left\{ \int_0^{1/\bar{\mu}} \frac{dk_x}{k_x} \left( \frac{k_x}{Q'} \right)^\epsilon - \int_0^Q \frac{dk_x}{k_x} \left( \frac{k_x}{Q'} \right)^\epsilon \cdot u \right\} \Big|_{\epsilon=0}, \quad (\text{B.39})$$

and optimise the choice of  $\bar{\mu}$  such that  $\Delta = \mathcal{O}(1)$ , i.e. it does not contain a  $\ln \nu$ -enhancement. Since  $\nu Q \gg 1$ , the second integral containing the exponential source function,  $u \propto \exp(-\nu k_x)$ , can be safely extended to infinity.

Evaluating the expression in the curly brackets up to  $\mathcal{O}(\epsilon)$ , we obtain

$$\begin{aligned} \left\{ \right\} &= \epsilon^{-1} \left[ (\bar{\mu} Q')^{-\epsilon} - \Gamma(1+\epsilon) (\nu Q')^{-\epsilon} \cdot \frac{1}{2} ((1-i\gamma y - i\beta)^{-\epsilon} + (1-i\gamma y + i\beta)^{-\epsilon}) \right] \\ &= -(\nu Q')^{-\epsilon} \left( \ln \frac{\bar{\mu}}{\nu} - \gamma_E - \frac{1}{2} \ln [(1-i\gamma y)^2 + \beta^2] + \mathcal{O}(\epsilon) \right). \end{aligned} \quad (\text{B.40})$$

Taking the  $\epsilon$ -derivative in (B.39) we obtain a large parameter  $\ln(\nu Q')$  accompanied by the factor which we set equal to zero to optimize the choice of  $\bar{\mu}$ :

$$\bar{\mu} = \nu e^{\gamma_E} \sqrt{(1-i\gamma y)^2 + \beta^2}. \quad (\text{B.41})$$

This means that, within SL accuracy, the source factor  $[1-u]$  can be substituted by

$$[1-u] \rightarrow \vartheta(k_x - \bar{\mu}^{-1}). \quad (\text{B.42})$$

Performing this substitution in (B.31) we get the result reported in the text, see (4.14).

## C. Evaluation of $\mathcal{F}$

The expression for  $\mathcal{F}_\delta$  is rather complicated. Invoking (4.5) we split the  $\gamma$ -integral into two pieces,

$$\mathcal{F} = \mathcal{F}_r + \mathcal{F}_i, \quad (\text{C.1})$$

namely the principal value and the  $\delta(\gamma)$  contributions,

$$\frac{1}{\gamma \mp i\epsilon} = \frac{P}{\gamma} \pm i\pi\delta(\gamma). \quad (\text{C.2})$$

We have

$$\mathcal{F} = \int_{-\infty}^{\infty} \frac{d\beta_2}{\pi(1+\beta_2^2)^{1+\frac{1}{2}C_2^{(\delta)}r'}} \int_{-\infty}^{\infty} \frac{d\beta_3}{\pi(1+\beta_3^2)^{1+\frac{1}{2}C_3^{(\delta)}r'}} \int_{-\infty}^{\infty} \frac{d\beta_1}{\pi} \cdot (\mathcal{I}_r + \mathcal{I}_i), \quad (\text{C.3})$$

where the two integrands are

$$\begin{aligned}\mathcal{I}_i &= \frac{1}{2} \left( \frac{1}{1+\beta_{12}^2} + \frac{1}{1+\beta_{13}^2} \right) \left( \sqrt{1+\beta_{12}^2} \sqrt{1+\beta_{13}^2} \right)^{\frac{C_1^{(\delta)} r'}{2}}, \\ \mathcal{I}_r &= \left( \frac{1}{1+\beta_{12}^2} - \frac{1}{1+\beta_{13}^2} \right) \int_0^\infty \frac{d\gamma}{\pi} \left( \sqrt{(1+\gamma)^2 + \beta_{12}^2} \sqrt{(1+\gamma)^2 + \beta_{13}^2} \right)^{\frac{-C_1^{(\delta)} r'}{2}} \frac{\sin(C_1^{(\delta)} r' A_1)}{\gamma}.\end{aligned}\quad (\text{C.4})$$

Here

$$A_1 = \frac{1}{2\pi} \int_0^\infty \frac{dx}{1-x^2} \left[ \ln \frac{(1+\gamma x)^2 + \beta_{12}^2}{(1+\gamma)^2 + \beta_{12}^2} - \ln \frac{(1+\gamma x)^2 + \beta_{13}^2}{(1+\gamma)^2 + \beta_{13}^2} \right] \quad (\text{C.5})$$

Where as before the colour factors are given by (B.33).

### C.1 $\mathcal{F}$ in the first order

In the  $\mathcal{O}(r')$  approximation we have, for  $\mathcal{F}_r$

$$\mathcal{F}_r(\bar{\nu}) \simeq C_1^{(\delta)} r' \int_{-\infty}^\infty \frac{d\beta_2}{\pi(1+\beta_2^2)} \int_{-\infty}^\infty \frac{d\beta_3}{\pi(1+\beta_3^2)} \int_{-\infty}^\infty \frac{d\beta_1}{\pi} \left( \frac{1}{1+\beta_{12}^2} - \frac{1}{1+\beta_{13}^2} \right) \frac{1}{\pi} \int_0^\infty \frac{d\gamma}{\gamma} A_1. \quad (\text{C.6})$$

Using

$$\frac{1}{\pi} \int_0^\infty \frac{d\gamma}{\gamma} A_1 = \frac{1}{8} \ln \frac{1+\beta_{12}^2}{1+\beta_{13}^2}, \quad (\text{C.7})$$

we find

$$\mathcal{F}_r(\bar{\nu}) \simeq \frac{r' C_1^{(\delta)}}{2} \int_{-\infty}^\infty \frac{d\beta_2}{\pi(1+\beta_2^2)} \int_{-\infty}^\infty \frac{d\beta_3}{\pi(1+\beta_3^2)} \int_{-\infty}^\infty \frac{d\beta_1}{2\pi} \left( \frac{1}{1+\beta_{12}^2} - \frac{1}{1+\beta_{13}^2} \right) \frac{1}{2} \ln \frac{1+\beta_{12}^2}{1+\beta_{13}^2}. \quad (\text{C.8})$$

Using

$$\int_{-\infty}^\infty \frac{d\beta}{\pi} \frac{\ln(1+\beta^2)}{1+\beta^2} = \ln 4. \quad (\text{C.9})$$

and

$$\int_{-\infty}^\infty \frac{d\beta_{13}}{\pi} \ln(1+\beta_{13}^2) \int_{-\infty}^\infty \frac{d\beta_{12}}{\pi(1+\beta_{12}^2)} \int_{-\infty}^\infty \frac{d\beta_1}{2\pi} \frac{1}{1+(\beta_{12}-\beta_1)^2} \frac{1}{1+(\beta_{13}-\beta_1)^2} = \ln 4. \quad (\text{C.10})$$

we obtain

$$\mathcal{F}_r(\bar{\nu}) \simeq -\frac{1}{2} \ln 4 \frac{C_1^{(\delta)}}{2} \cdot r'(\bar{\nu}). \quad (\text{C.11})$$

Expanding  $\mathcal{F}_i$  in  $r'$  we obtain in the first order:

$$\begin{aligned} \mathcal{F}_i(\bar{\nu}) = 1 - \frac{1}{2}r' \cdot \int_{-\infty}^{\infty} \frac{d\beta_2}{\pi(1+\beta_2^2)} \int_{-\infty}^{\infty} \frac{d\beta_3}{\pi(1+\beta_3^2)} \int_{-\infty}^{\infty} \frac{d\beta_1}{2\pi} \left( \frac{1}{1+\beta_{12}^2} + \frac{1}{1+\beta_{13}^2} \right) \\ \left( C_2^{(\delta)} \ln(1+\beta_2^2) + C_3^{(\delta)} \ln(1+\beta_3^2) + \frac{1}{2}C_1^{(\delta)} [\ln(1+\beta_{12}^2) + \ln(1+\beta_{13}^2)] \right) \end{aligned} \quad (\text{C.12})$$

Using (C.9) and (C.10) we get:

$$\mathcal{F}_i(\bar{\nu}) = 1 - \frac{1}{2} \ln 4 \left( \frac{3}{2}C_1^{(\delta)} + C_2^{(\delta)} + C_3^{(\delta)} \right) \cdot r'(\bar{\nu}). \quad (\text{C.13})$$

So, in the first order,

$$\mathcal{F} = \mathcal{F}_r(\bar{\nu}) + \mathcal{F}_i(\bar{\nu}) = 1 - \frac{1}{2} \ln 4 \left( 2C_1^{(\delta)} + C_2^{(\delta)} + C_3^{(\delta)} \right) \cdot r'(\bar{\nu}) \quad (\text{C.14})$$

## References

- [1] S. Catani, L. Trentadue, G. Turnock and B.R. Webber, *Nucl. Phys.* **B 407** (1993) 3.
- [2] S. Catani and B.R. Webber, *Phys. Lett.* **B 427** (1998) 377 [hep-ph/9801350].
- [3] S. Catani, G. Turnock and B.R. Webber, *Phys. Lett.* **B 295** (1992) 269;  
Yu.L. Dokshitzer, A. Lucenti, G. Marchesini and G.P. Salam, *J. High Energy Phys.* **01** (1998) 011  
[hep-ph/9801324].
- [4] V. Antonelli, M. Dasgupta and G.P. Salam, *J. High Energy Phys.* **02** (2000) 001  
[hep-ph/9912488].
- [5] M. Beneke, *Phys. Rep.* **317** (1999) 1 [hep-ph/9807443];  
B.R. Webber, *Nucl. Phys.* **71** (Proc. Suppl.) (1999) 66 [hep-ph/9712236].
- [6] Yu.L. Dokshitzer, *Perturbative QCD and Power Corrections*, Invited talk at 11th Rencontres de Blois: Frontiers of Matter, Chateau de Blois, France, 28 Jun – 3 Jul 1999 [hep-ph/9911299].
- [7] B.I. Ermolayev and V.S. Fadin, *Sov. Phys. JETP Lett.* **33** (1981) 269;  
A.H. Mueller, *Phys. Lett.* **B 104** (1981) 161.
- [8] Yu.L. Dokshitzer and S.I. Troyan, “*Asymptotic freedom and Local Parton-Hadron Duality in QCD jet physics*”, Proceedings of 19th Leningrad Winter School, Leningrad 1984, p. 144; for review see Yu.L. Dokshitzer, V.A. Khoze, A.H. Mueller and S.I. Troyan, “*Basics of Perturbative QCD*”, ed. J. Tran Thanh Van, Editions Frontières, Gif-sur-Yvette, 1991;  
A.H. Mueller, *Nucl. Phys.* **B 213** (1983) 85, Erratum quoted *ibid.* **B 241** (1984) 141;  
E.D. Malaza and B.R. Webber, *Phys. Lett.* **B 149** (1984) 501.

- [9] Yu.L. Dokshitzer, S.I. Troyan and V.A. Khoze, *Sov. J. Nucl. Phys.* **46** (1987) 712.
- [10] A. Banfi, G.P. Salam and G. Zanderighi, work in progress.
- [11] L3 Collaboration, B. Adeva et al., *Z. Physik C* **55** (1992) 39;  
D.P. Barber, et al., *Phys. Lett. B* **89** (1979) 139.
- [12] Yu.L. Dokshitzer, G. Marchesini and G.P. Salam, *Eur. Phys. J. C* **3** (1999) 1  
[hep-ph/9812487].
- [13] A. Banfi, Yu.L. Dokshitzer, G. Marchesini and G. Zanderighi, under preparation.
- [14] S. Catani and M. Grazzini, [hep-ph/9908523]
- [15] A. Banfi, Yu.L. Dokshitzer, G. Marchesini and G. Zanderighi, under preparation.
- [16] Yu.L. Dokshitzer, A. Lucenti, G. Marchesini and G.P. Salam, *Nucl. Phys. B* **511** (1998) 396 [hep-ph/9707532].
- [17] S. Catani, G. Marchesini and B.R. Webber, *Nucl. Phys. B* **349** (1991) 635.
- [18] Yu.L. Dokshitzer, A. Lucenti, G. Marchesini and G.P. Salam, *J. High Energy Phys.* **05** (1998) 003  
[hep-ph/9802381];  
M. Dasgupta and B.R. Webber, *J. High Energy Phys.* **10** (1998) 001 [hep-ph/9809247].
- [19] V.A. Khoze and W. Ochs, *Int. J. Mod. Phys. A* **12** (1997) 2949 [hep-ph/9701421].